THE JOURNAL OF BIOLOGICAL CHEMISTRY VOL. 288, NO. 41, pp. 29846–29861, October 11, 2013

Co-existence of Distinct Prion Types Enables Conformational Evolution of Human PrP^{Sc} by Competitive Selection*

Received for publication, July 9, 2013, and in revised form, August 5, 2013 Published, JBC Papers in Press, August 23, 2013, DOI 10.1074/jbc.M113.500108

Tracy Haldiman[‡], Chae Kim[‡], Yvonne Cohen[‡§], Wei Chen[‡§], Janis Blevins[‡§], Liuting Qing[‡], Mark L. Cohen[‡§], Jan Langeveld[¶], Glenn C. Telling[‖], Qingzhong Kong[‡], and Jiri G. Safar[‡§**1]**

*From the Departments of [‡]Pathology and **Neurology and [§]National Prion Disease Pathology Surveillance Center, School of Medicine, Case Western Reserve University, Cleveland, Ohio 44106, the [¶]Central Veterinary Institute of Wageningen UR, 8200 AB Lelystad, The Netherlands, and the [‖]Department of Microbiology, Immunology, and Pathology, Colorado State University, Fort Collins, Colorado 80523-1619*

Background: Mechanism of prion adaptation and evolution has not been fully elucidated.
Results: Distinct human prion particles co-exist and undergo competitive selection during replication.
Conclusion: The process is governed by preferential replication of the least stable pathogenic conformers.
Significance: The spectrum of conformers in wild human prion isolates enables adaptation and evolution by selection of the progressively less stable and faster replicating subset.

The unique phenotypic characteristics of mammalian prions are thought to be encoded in the conformation of pathogenic prion proteins (PrP^{Sc}). The molecular mechanism responsible for the adaptation, mutation, and evolution of prions observed in cloned cells and upon crossing the species barrier remains unsolved. Using biophysical techniques and conformation-dependent immunoassays in tandem, we isolated two distinct populations of PrP^{Sc} particles with different conformational stabilities and aggregate sizes, which frequently co-exist in the most common human prion disease, sporadic Creutzfeldt-Jakob disease. The protein misfolding cyclic amplification replicates each of the PrP^{Sc} particle types independently and leads to the competitive selection of those with lower initial conformational stability. In serial propagation with a nonglycosylated mutant PrP^{C} substrate, the dominant PrP^{Sc} conformers are subject to further evolution by natural selection of the subpopulation with the highest replication rate due to its lowest stability. Cumulatively, the data show that sporadic Creutzfeldt-Jakob disease PrP^{Sc} is not a single conformational entity but a dynamic collection of two distinct populations of particles. This implies the co-existence of different prions, whose adaptation and evolution are governed by the selection of progressively less stable, faster replicating PrP^{Sc} conformers.

Ample genetic, transgenetic, and biophysical data, and ultimately the generation of infectious prions from recombinant prion protein (PrP)[2] *in vitro* (1–3) all provide compelling evidence that prion diseases are caused by the accumulation of an aberrantly folded isoform of the prion protein termed PrP^{Sc} (4). Variations in prions, which cause remarkably different disease phenotypes in the same host, are referred to as strains (5, 6). For several decades, the existence of distinct prion strains that can be passaged indefinitely has polarized the scientific community and was offered as an argument for the existence of a prion-specific genome. Subsequently, extraordinary progress in the past decade has produced convincing experimental evidence indicating that the species of prion is encoded in the primary amino acid sequence of PrP^{Sc} (6) and that prion strain characteristics are encoded in the self-replicating conformation of PrP^{Sc} (7–10). These phenotypic characteristics may undergo mutation in cloned cells, but the molecular mechanism responsible for this phenomenon remained elusive in the absence of informative nucleic acid (10). Although recent important experiments with synthetic and rodent-adapted laboratory prions suggest that structural plasticity of PrP^{Sc} is a key factor in adaptation and evolution, the exact conformational mechanism and relevancy of these observations to wild prions causing natural human prion diseases have not been established (11–13).

The extensive phenotypic heterogeneity of the most frequent human prion disease, sporadic Creutzfeldt-Jakob disease (sCJD) (14), is currently understood as a complex interplay between polymorphisms in the *PRNP* gene and different PrP^{Sc} conformers (6, 14). Because the conformations of PrP^{Sc} vary in different prion strains, the broad spectrum of distinct PrP^{Sc} conformers recently found in different cases of sCJD using sensitive biophysical techniques implies that sCJD is caused by a broad array of distinct prions (5, 15, 16). Furthermore, the fre-

* This work was supported, in whole or in part, by National Institutes of Health Grant NS074317. This work was also supported by Centers for Disease Control and Prevention Grant UR8/CCU515004 and the Charles S. Britton Fund.

[1] To whom correspondence should be addressed: Dept. of Pathology, Case Western Reserve University, 2085 Adelbert Rd., Cleveland, OH 44106. Tel.: 216-368-4609; Fax: 216-368-4090; E-mail: jiri.safar@case.edu.

[2] The abbreviations used are: PrP, prion protein; CDI, conformation-dependent immunoassay; MM1 sCJD, sporadic Creutzfeldt-Jakob disease homozygous for methionine in polymorphic codon 129 of *PRNP* gene and 21-kDa fragment (type 1) of unglycosylated $rPrP^{Sc}$ on WB; MM2 sCJD, sporadic Creutzfeldt-Jakob disease homozygous for methionine in polymorphic codon 129 of *PRNP* gene and 19-kDa fragment (type 2) of unglycosylated $rPrP^{Sc}$ on WB; *PRNP*, prion protein gene; PrP^{C}, normal or cellular prion protein; PrP^{Sc}, misfolded pathogenic prion protein; $rPrP^{Sc}$, protease-resistant conformers of pathogenic prion protein (PrP(27–30)); sPMCA, serial protein misfolding cyclic amplification; $sPrP^{Sc}$, protease-sensitive conformers of pathogenic prion protein; PMCA, protein misfolding cyclic amplification; WB, Western blot; PK, proteinase K; TRF, time-resolved fluorescence; Tg, transgenic.

quent, and perhaps universal, presence of both the 21-kDa (type 1) and 19-kDa (type 2) unglycosylated fragments of protease-resistant (r) PrP^{Sc} in sCJD (17–21) indicates the co-occurrence of markedly different PrP^{Sc} conformers, often in the same anatomical structure in the same brain. Apart from challenging the validity of the clinicopathological classification of sCJD based on *PRNP* gene polymorphism and Western blot patterns of type 1 or type 2 rPrP^{Sc} (14, 22), these findings raise some fundamental questions. (*a*) Do the co-existent type 1 and type 2 rPrP^{Sc} form distinct or hybrid particles composed of both types of PrP^{Sc}? (*b*) Do they replicate independently and thus imply co-existence of different sCJD prions? (*c*) What is the impact of co-existence of distinct PrP^{Sc} conformers on prion adaptation and evolution?

In our earlier experiments, we found a remarkable inter-individual conformational heterogeneity of sCJD PrP^{Sc}, and we established that progression rates of the disease correlate with replication rate of human prions *in vitro*, which is in turn governed by the size and instability of aggregates formed by this protein (6, 15, 16). To extend these observations with the aim to advance our understanding of the molecular mechanism of human prion co-existence, adaptation, and evolution, we applied complementary biophysical techniques to a set of representative sCJD cases with the co-occurrence of type 1 and type 2 rPrP^{Sc} (type 1 + 2) in the same cortical location (20) in the same brain. First, we investigated whether sCJD with mixed type 1 + 2 sCJD PrP^{Sc} would contain a single particle composed of conformers that generate two different fragments after proteolytic digestion or whether they represent the distinct prion particles expected for different prions (15). We isolated two distinct prion particle populations that display differing conformational stabilities and different sedimentation velocities in the sucrose gradient, which argues that the co-occurrence of type 1 and 2 PrP^{Sc} in sCJD is due to the presence of two distinct aggregates, each containing a subpopulation of similar conformers of PrP^{Sc}. The independent replication of type 1 and type 2 PrP^{Sc} populations with markedly different replication rates in sPMCA argues for the co-existence of different prions in the same sCJD brain. The invariable and progressive dominance of type 1 PrP^{Sc} and the subsequent disappearance of type 2 from the mixture during serial amplification suggest a competition between different conformers and ongoing conformational evolution through the natural selection of faster replicating PrP^{Sc} conformers.

MATERIALS AND METHODS

Ethics Statement—All procedures were performed under protocols approved by the Institutional Review Board at Case Western Reserve University. In all cases, written informed consent for research was obtained from the patient or legal guardian, and the material used had appropriate ethical approval for use in this project. All patients' data and samples were coded and handled according to National Institutes of Health guidelines to protect the patients' identities.

sCJD Cases—We selected six representative subjects with a mixed pattern of rPrP^{Sc} on Western blots of brain tissue from a group of 36 patients with a definitive diagnosis of sCJD. The criteria for inclusion were as follows: (*a*) availability of clinical diagnosis of CJD according to World Health Organization criteria (23–25); (*b*) methionine homozygous at codon 129 of the human prion protein (PrP) gene (*PRNP*); (*c*) unequivocal WB classification; (*d*) unequivocal classification of pathology as sCJD at the National Prion Disease Pathology Surveillance Center in Cleveland, OH; (*e*) demographic data distribution within the 95% confidence interval of the whole sCJD group, resulting in no difference between selected cases and the whole group in any of the statistically followed parameters.

Brain Samples and PRNP Gene Sequencing—DNA was extracted from frozen brain tissues in all cases, and genotypic analysis of the *PRNP* coding region was performed as described (26–28). Patients lacked pathogenic mutations in the *PRNP* and had no history of familial diseases or known exposure to prion agents. These cases underwent additional detailed WB analyses of the PrP^{Sc} so that we could ascertain the accuracy of their original classification and confirm that the same brain homogenate analyzed by CDI contained mixed type 1 + 2 PrP^{Sc}(129M). Coronal sections of human brain tissues were obtained at autopsy and stored at −80 °C. Three 200–350-mg cuts of frontal (superior and more posterior middle gyri) or occipital cortex were taken from each brain and used for molecular analyses.

Brain Homogenates—Slices of tissues weighing 200–350 mg were first homogenized to a final 15% (w/v) concentration in calcium- and magnesium-free PBS, pH 7.4, by three 75-s cycles with Mini-beadbeater 16 Cell Disrupter (Biospec, Bartlesville, OK). The homogenates were then diluted to a final 5% (w/v) in 1% (v/v) Sarkosyl in PBS, pH 7.4, and rehomogenized. After clarification at 500 × *g* for 5 min, 1 aliquot of the supernatant was treated with protease inhibitors (0.5 mM PMSF and aprotinin and leupeptin at 5 μg/ml, respectively). The second aliquot was treated with 50 μg/ml of proteinase K (Amresco, Solon, OH) for 1 h at 37 °C and shaking 600 rpm on an Eppendorf Thermomixer (Eppendorf, Hauppauge, NY), and PK was blocked with PMSF and aprotinin/leupeptin mixture.

Western Blots—Both PK-treated and -untreated samples were diluted 9-fold in 1× Laemmli Buffer (Bio-Rad) containing 5% (v/v) β-mercaptoethanol and a final 115 mM Tris-HCl, pH 6.8. Samples were heated for 5 min at 100 °C, and ~2 ng of PrP per lane was loaded onto 15% Tris-HCl, SDS-polyacrylamide gels (Bio-Rad) mounted in Western blot apparatus (Bio-Rad). After electrotransfer to Immobilon-P transfer membranes (Millipore, Bedford, MA), the membranes were blocked with 2% (w/v) BSA in TBS containing 0.1% of Tween 20 (v/v) and 0.05% (v/v) Kathon CG/ICP (Sigma). The PVDF membranes were developed with 0.05 μg/ml biotinylated mAb 3F4 (Covance, Princeton, NJ) followed by 0.0175 μg/ml streptavidin-peroxidase conjugate (Fisher) or with ascitic fluid containing mAb 3F4 (kindly supplied by Richard Kascsak) diluted 1:20,000 followed by peroxidase-labeled sheep anti-mouse IgG Ab (Amersham Biosciences) and diluted 1:3000. Alternatively, the membranes were developed with mAb 12B2 (29) for detection of type 1 rPrP^{Sc} or mAb 1E4 (30) for detection of type 2 rPrP^{Sc}, respectively. The membranes were developed with the ECL Plus detection system (Amersham Biosciences) and exposed to Kodak BioMax MR films (Fisher) or Kodak BioMax XAR films (Fisher).

Conformation-dependent Immunoassay—The CDI for human PrP was performed as described previously (28, 31), with several modifications. First, we used white Lumitrac 600 High Binding Plates (E&K Scientific, Santa Clara, CA) coated with mAb 8H4 (epitope 175–185) (32) in 200 mM NaH_2PO_4 containing 0.03% (w/v) NaN_3, pH 7.5. Second, aliquots of 20 μl from each fraction containing 0.007% (v/v) of Patent Blue V (Sigma) were directly loaded into wells of white strip plates prefilled with 200 μl of Assay Buffer (PerkinElmer Life Sciences). Finally, the captured PrP was detected by a europium-conjugated (9) anti-PrP mAb 3F4 (epitope 108–112) (33) or europium-labeled mAb 12B2 (29), and the time-resolved fluorescence (TRF) signals were measured by the multimode microplate reader PHERAstar Plus (BMG LabTech, Durham, NC). The recHuPrP(90–231,129M) and PrP(23–231,129M) used as a calibrant in the CDI was a gift from Witold Surewicz, and preparation and purification have been described previously (34). The initial concentration of recombinant human PrP(23–231) and PrP(90–231) was calculated from absorbance at 280 nm and molar extinction coefficients 56,650 and 21,640 $M^{-1}cm^{-1}$, respectively. The purified recombinant proteins were dissolved in 4 M GdnHCl and 50% Stabilcoat (SurModics, Eden Prairie, MN) and stored at −80 °C. The concentration of PrP was calculated from the CDI signal of denatured samples using calibration curve prepared with either recPrP(23–231) for samples containing full-length PrP^{Sc} or recPrP(90–231) for samples containing truncated rPrP^{Sc} (PrP(27–30)) after proteinase K treatment.

The calibration and validation of CDI has been published extensively by us and others (15, 16, 28, 35–41). Briefly, the PK-untreated sample containing PrP was divided into native and denatured aliquots, and the latter was denatured with 4 M GdnHCl for 5 min at 80 °C. Using europium-labeled mAb 3F4 for detection, the TRF signal of the native sample corresponded to epitope 107–112 that was exposed in α-helical PrP^{C} and hidden in PrPSc and is proportional to the concentration of PrPC (37). The signal of the denatured aliquot corresponded to the total PrP in a sample, and the concentration of PrPSc was then calculated according to the following: $[PrP^{Sc}] = [PrP_D] - [PrP_N]$. Next, the concentration of protease-resistant rPrPSc was calculated in samples subjected to the protease K treatment followed by complete denaturation using the PrP(90–231) calibration curve. The concentration of sPrPSc was calculated according to the following: $[sPrP^{Sc}] = [PrP^{Sc}] - [rPrP^{Sc}]$. The separate calibration for PK-treated and -untreated samples was critical for correct results due to the ~3.5-fold lower affinity of mAb 3F4 with denatured full-length human PrP(23–231,129M) compared with PrP(90–231,129M) (15, 16).

Monitoring Dissociation and Unfolding of PrP^{Sc} by CDI—The denaturation of human PrP^{Sc} was performed as described previously (9), with several modifications. Frozen aliquots of PrP^{Sc} were thawed, sonicated three times for 5 s at 60% power with Sonicator 4000 (Qsonica, Newtown, CT), and the concentration was adjusted to a constant ~50 ng/ml PrP^{Sc}. The 15-μl aliquots in 15 tubes were treated with increasing concentrations of 8 M GdnHCl containing 0.007% (v/v) Patent Blue V (Sigma) in 0.25 M or 0.5 M increments. After a 30-min incubation at room temperature, individual samples were rapidly diluted with Assay Buffer (PerkinElmer Life Sciences) containing diminishing concentrations of 8 M GdnHCl, so that the final concentration in all samples was 0.411 M. Each individual aliquot was immediately loaded in triplicate to dry white Lumitrac 600, High Binding Plates (E&K Scientific, Santa Clara, CA), coated with mAb 8H4, and developed in accordance with CDI protocol using europium-labeled mAb 3F4 or 12B2 for detection (9, 28, 36, 42).

The raw TRF signal was converted into the apparent fractional change of unfolding (F_{app}) as follows: $F = (TRF_{OBS} - TRF_N)/(TRF_U - TRF_N)$, where TRF_{OBS} is the observed TRF value, and TRF_N and TRF_U are the TRF values for native and unfolded forms, respectively, at the given GdnHCl concentrations (43). To determine the concentration of GdnHCl where 50% of PrP^{Sc} is unfolded ($[GdnHCl]_{1/2}$), the data were fitted by the least square method with a sigmoidal transition model (Equation 1),

$$F_{app} = F_0 + \frac{(F_{max} - F_0)}{1 + e^{\{(c_{1/2} - c)/r\}}} \quad \text{(Eq. 1)}$$

The apparent fractional change (F) in the TRF signal is the function of GdnHCl concentration (c); $c_{1/2}$ is the concentration of GdnHCl at which 50% of PrP^{Sc} is dissociated/unfolded, and r is the slope constant. To determine the impact of protease treatment on the conformational stability of PrP^{Sc}, the values of fractional change after PK were subtracted from F_{app} values obtained before PK ($\Delta F_{app} = F^0 - F^{PK}$) and then fitted with a Gaussian model to estimate the proportion and average stability of sPrP^{Sc} conformers (Equation 2),

$$\Delta F_{app} = F_0 + A^{\{-(c - c_0)^2\}} \quad \text{(Eq. 2)}$$

In this model, the PK-induced fractional change is ΔF; F_0 is the fractional change at 0 concentration of GdnHCl, and c_0 is the GdnHCl concentration at the maximum height A of the peak.

Sucrose Gradient Ultracentrifugation—The 400-μl aliquots of 10% brain homogenate in PBS, pH 7.4, containing 2% Sarkosyl were clarified by centrifugation at 500 × g for 5 min and carefully layered onto the top of the 10–45% sucrose gradient. The sucrose gradient was prepared in PBS, pH 7.4, containing 1% Sarkosyl in thin wall polyallomer (13 × 51 mm) tubes (Beckman Instruments, Palo Alto, CA). Alternatively, the brain homogenates and sucrose gradients destined for PMCA were prepared in 1% Triton X-100. The ultracentrifugation was performed at 50,000 rpm for 73 min at 5 °C in an Optima TL ultracentrifuge (Beckman Instruments) equipped with an SW 55 Ti rotor (Beckman Instruments). After the centrifugation, the 200- or 400-μl fractions of gradients were collected from the bottom of the tube and assayed for PrP by CDI and WBs. The densitometry of WBs was performed with ImageJ software. To compare the sucrose gradient profiles of different PrPs developed with different antibodies, the raw data were converted to apparent fractional change according to the following: $F_{app} = (D_{OBS} - D_{min})/(D_{max} - D_{min})$ where D_{OBS} is the observed D value, and D_{max} and D_{min} are the density values for fractions with maximum and minimum values, respectively, at the given sucrose fraction.

Nonglycosylated Mutated Human PrP^{C}(129M) Substrate Used in PMCA of sCJD PrP^{Sc}—The human PrP$^{N181Q/N197Q}$ ORF, which contains two point mutations that change Asn to Gln at positions 181 and 197, thereby eliminating the two *N*-linked glycosylation sites on human PrP, was generated by PCR mutagenesis from the human PrP-129M transgene construct used for the generation of the Tg40 mice and described previously (44). The human PrP$^{N181Q/N197Q}$ transgene construct was then generated by inserting the human PrP$^{N181Q/N197Q}$ ORF into the NruI site of the pHGD3 plasmid that was made by replacing the mouse PrP ORF in the half-genomic PrP clone (pHGPRP) with the restriction sites for ClaI and NruI (44). The transgene construct was microinjected into fertilized FVB/NJ eggs and planted into the oviducts of pseudo-pregnant CD-1 mice to obtain TgPrP$^{N181Q/N197Q}$ founder pups. All TgPrP$^{N181Q/N197Q}$ founder mice were bred with FVB/Prnp0/0 mice (45) to obtain TgPrP$^{N181Q/N197Q}$ mice in the mouse PrP-null background. Several TgPrP$^{N181Q/N197Q}$ lines were obtained, and the TgPrP$^{N181Q/N197Q}$ line was bred to homozygosity to generate the TgNN6h mice, whose human PrP$^{N181Q/N197Q}$ expression level in the brain is about 60% of the PrP level found in wild type FVB mice based on CDI analysis using monoclonal antibody 12B2 in CDI (Fig. 6, *A* and *B*). Perfused brain tissues from the TgPrP$^{N181Q/N197Q}$ mice homogenized in PBS, pH 7.4, containing 1% Triton X-100, 5 mM EDTA, and protease inhibitor mixture (Roche Applied Science) were used as substrates for PMCA.

Protein Misfolding Cyclic Amplification (PMCA)—Sonication-driven PMCA was performed as described previously (15, 46) with the following modifications. The PrP^{Sc} was replicated using brains of transgenic mice expressing unglycosylated human PrP$^{N181Q/N197Q}$ with methionine at position 129 (44). Brain homogenates from infected mice or the human type MM1 sCJD case were diluted as described in the specific experiments to attain a final 10% brain homogenate, and 60 μl was transferred into 0.2 ml of PCR tubes equipped with 2.38 mm diameter PTFE ball (K-mac Plastics, Wyoming, MI). The buffer in all PMCA reactions was PBS, pH 7.4, containing a final 1% Triton X-100, 500 mM NaCl, 0.1% Sarkosyl, and 1 mM of an antioxidant α-tocopherol. Tubes were positioned on an adaptor placed on the plate holder of a microsonicator (Misonix Model 3000, Farmingdale, NY) and programmed to perform cycles of 60 min of incubation at 35 °C followed by a 30-s pulse of sonication set at 80% power. Samples were incubated, without shaking, and immersed in the water of the sonicator bath for 48 cycles. The 30 μl of the amplified materials were transferred to the next tube prefilled with 30 μl of substrate brain homogenate for the next round, and the remaining 30-μl aliquot was analyzed with CDI and WBs.

RESULTS

Measurement of Type 1 + 2 and Type 1 PrP^{Sc} in sCJD Cortex with CDI—Based on a previous study of 36 cases with mixed type 1 + 2 rPrP^{Sc} (20), we selected six cases with a co-occurrence of type 1 + 2 rPrP^{Sc} in the same cortical location for detailed investigation. All cases were methionine homozygous at codon 129 (MM) of the human PrP gene (*PRNP*) and had a definitive diagnosis of sCJD at the National Prion Disease Pathology Surveillance Centre in Cleveland, OH. The mixed type 1 + 2 rPrP^{Sc} were found either in the frontal (n = 3) or occipital (n = 3) cortex. All cases lacked pathogenic mutations in the *PRNP* and had no history of familial diseases or known exposure to prions. The presence of mixed type 1 + 2 rPrP^{Sc} was verified using the recommended conditions (20, 47) and high resolution gels, to verify the accuracy of their original classification as sCJD type 1 + 2 (Fig. 1*A*). The descriptive demographics indicate that these cases are representative of the whole mixed type 1 + 2 group reported previously (20) and are similar to mixed type 1 + 2 cases reported by others (Table 1) (20, 48, 49).

To measure the concentration of total type 1 + 2 PrP^{Sc}, protease-resistant fraction (rPrP^{Sc}), and protease-sensitive fraction (sPrP^{Sc}) in the brain cortex, we used europium-labeled mAb 3F4 (epitope 107–112) (33) for detection, and 8H4 mAb (epitope residues 175–185) (32) to capture human PrP^{Sc} in a sandwich CDI format (Fig. 1*B*) (28, 31). The concentration of PrP was calculated from the CDI signal of completely GdnHCl-denatured samples using a calibration curve prepared with either denatured human recPrP(23–231) for samples containing full-length PrP^{Sc} or recPrP(90–231) for samples containing truncated rPrP^{Sc} (PrP(27–30)) after proteinase K treatment. As we reported previously, this separate calibration is necessary due to the ~3.5-fold lower affinity of mAb 3F4 with full-length human PrP(23–231,129M) compared with PrP(90–231,129M) (15, 16). The analytical sensitivity and specificity of the optimized CDI for the detection of both sPrP^{Sc} and rPrP^{Sc} using europium-labeled mAb 3F4 were previously reported by us and others (9, 28, 36, 39).

For the selective measurement of denatured type 1 rPrP^{Sc} after PK treatment, we developed a sandwich CDI using europium-labeled mAb 12B2 (epitope 89–93) to detect and 8H4 mAb (epitope residues 175–185) (32) to capture human rPrP^{Sc} type 1. The sandwich CDI with europium-labeled mAb 12B2 has a detection sensitivity of full-length denatured recombinant human PrP(23–231) comparable with europium-labeled 3F4 (Fig. 1*C*) (16, 28). In contrast to mAb 3F4, the mAb 12B2 does not detect shorter fragments of denatured PrP starting at residue ~90 (Fig. 1*C*). The serial dilutions of brain homogenates obtained from "pure" sCJD with MM1, MM2, and VV2 PrP^{Sc} demonstrate sensitivity and specificity of detection of denatured full-length PrP^{Sc} similar to europium-labeled 3F4 (Fig. 1*D*). After protease K treatment, the type 1 PrP^{Sc} present in MM1 sCJD was detected with the same end point sensitivity as with mAb 3F4 (16, 28). Even though the MM2 and VV2 cases did not show any residual type 1 PrP on Western blots, and were considered pure type 2, the CDI with mAb 12B2 demonstrated low levels of type 1 PrP^{Sc} that are equivalent to ~1% of total rPrP^{Sc} (Fig. 1*E*).

To expand these findings, we tested 36 sCJD cases that were classified with WBs as pure MM1 (n = 10), mixed type 1 + 2 cases (n = 6), MM2 (n = 10), and VV2 (n = 10) sCJD. Based on CDI monitoring rPrP^{Sc} with both 3F4 and 12B2 antibodies, we detected in each group a variable proportion of both type 1 and type 2 components (Fig. 2*A*). The content of type 1 rPrP^{Sc} in the MM2 WB group varied between 0.6 and 20% and in the VV2 WB group between 4 and 20% (Fig. 2*B*). From these experiments, we concluded that the sandwich CDI with europium-labeled mAb 12B2 detects type 1 rPrP^{Sc} with high sensitivity

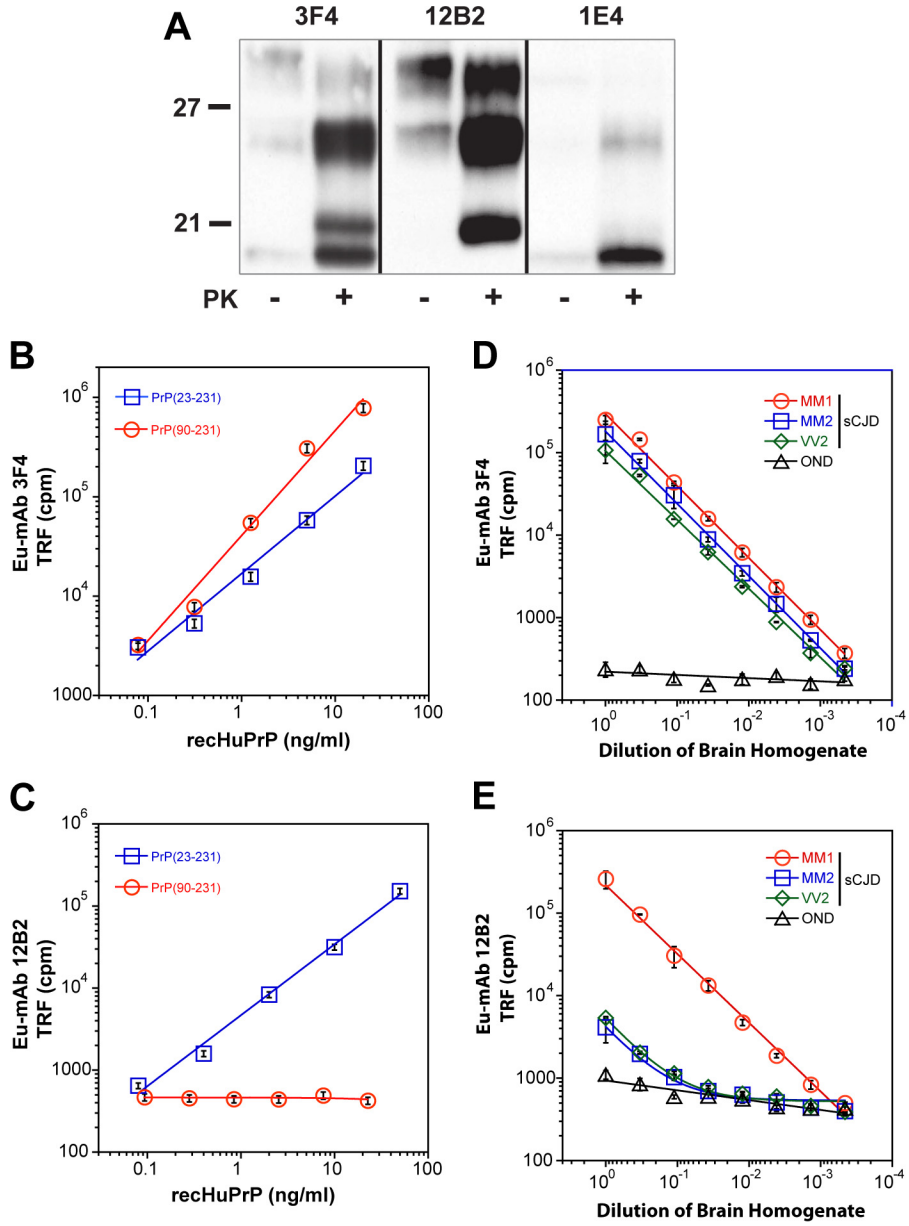

FIGURE 1. **Western blot specificity and calibration of CDI using mAb 3F4 and 12B2.** *A*, WB pattern of typical sCJD with mixed type 1 + 2 PrP^{Sc} before and after proteinase K (*PK*) treatment. The WB was developed with monoclonal antibody 3F4 (epitope 107–112) reacting with the doublet of both 21- and 19-kDa bands of unglycosylated rPrP^{Sc}, 12B2 (epitope 89–93) reacting preferentially with 21-kDa band (type 1), and 1E4 (epitope 97–108) reacting preferentially with type 2 rPrP^{Sc}. The molecular mass of the standard proteins is in kDa. *B* and *C*, calibration of CDI with (*blue squares*) full-length (PrP(23–231,129M)) or (*red circles*) truncated (PrP(90–231,129M)) human prion protein and detected with europium-labeled mAb 3F4 (*B*) or with Europium-labeled mAb 12B2 (*C*). *D* and *E*, sensitivity and specificity of type 1 rPrP^{Sc} detection with CDI using europium-labeled mAb 12B2. The different cases of sCJD that were classified pure after diagnostic WBs and a case of other neurological disorders (*OND*) were serially diluted and tested with CDI using europium-labeled mAb 3F4 (*D*) or europium-labeled mAb 12B2 (*E*). To obtain optimum discrimination of type 1 from type 2 rPrP^{Sc}, samples were treated with PK at a concentration equivalent to 3 IU/ml (100 μg/ml) of 10% brain homogenate for 1 h at 37 °C and precipitated with phosphotungstic acid after blocking PK with the protease inhibitor mixture. The 8H4 mAb was used for capture of denatured PrP^{Sc}. *Data points* and *bars* represent average ± S.D. obtained from three or four independent measurements.

and specificity. The low but reproducible levels of type 1 PrP^{Sc} we observed in type 2 sCJD cases with different polymorphisms in the *PRNP* gene confirmed the data obtained with different techniques and antibodies by others (17–19, 21) and indicated that the presence of both types of rPrP^{Sc} in the same sCJD case is a universal phenomenon.

Protease Sensitivity and Conformational Stability of Type 1 + 2 rPrP^{Sc}—The CDI allows a differentiation of PrP^{Sc} from PrPC without PK treatment, and after calibration with human recPrP(23–231), a reliable measurement of total PrP^{Sc} (15, 16, 28, 35–37). The CDI has been now introduced in numerous other laboratories (38–41), and by measuring the concentration of completely denatured PrP^{Sc} before and after PK treatment, this allowed us to determine the levels of the prion strain-specific protease-sensitive (see under "Materials and Methods" for detail explanation) PrP^{Sc} (6, 15, 16, 37). Measured with CDI, the sCJD cases with mixed type 1 + 2 rPrP^{Sc} in the same location, and homozygous for methionine in codon 129 of the

TABLE 1
Descriptive statistics of the data and demographics of sCJD cases

PRNP codon 129	MM											
WB type	1+2											
Variable	Units	n	Minimum	Maximum	Mean	±	S.E.M.	Minimum	Maximum	Mean	±	S.E.M.
Sex	F/M	4/2										
Age	years	6	51	74	62.5	±	3.5					
Disease Duration	month	5	3.2	22.2	8.0	±	3.3					
Detection Antibody in CDI		6	3F4					12B2				
PrP^{Sc}	ng/ml	6	121	579	353	±	81	135	442	290	±	52
PrP^{Sc} Gdn HCl$_{1/2}$	M	6	2.69	3.11	2.93	±	0.06	2.57	3.01	2.85	±	0.07
rPrP^{Sc}	ng/ml	6	53	198	113	±	23	19	45	31	±	5
rPrP^{Sc} Gdn HCl$_{1/2}$	M	6	2.56	3.34	2.84	±	0.11	2.96	3.21	3.09	±	0.05
rPrP^{Sc} Type 1	%	6	12	69	36	±	10	12	69	36	±	10
sPrP^{Sc}	ng/ml	6	68	426	240	±	60	101	419	259	±	55
sPrP^{Sc}	%	6	56	77	66	±	3	71	95	86	±	4
PK-induced Change in Stability	Δ Fapp	6	-0.36	0.34	-0.10	±	0.11	0.02	0.59	0.24	±	0.08

PRNP gene, had variable levels of PrP^{Sc}, and the levels of sPrP^{Sc} varied from 55 to 80% in individual cases (Table 1 and Fig. 2, *C* and *D*). The type 1 rPrP^{Sc} content varied in individual cases from 12 to 69% of the total rPrP^{Sc}, with complementary type 2 levels between 31 and 88% (Fig. 2*D*). We observed wide inter-individual variations in stabilities of PrP^{Sc}, and the stabilities of total PrP^{Sc} measured with either mAb 3F4 or mAb 12B2 (Fig. 2*E*) were similar. In contrast to the variable response of PrP^{Sc} stability to PK treatment when followed with mAb 3F4, we observed a remarkably uniform increase in stability of all cases with mAb 12B2. In general, the stabilities of rPrP^{Sc} obtained with mAb 12B2 were significantly higher than those obtained with mAb 3F4. Because the unfolding curves obtained with mAb 3F4 reflect the unfolding of both type 1 and type 2 rPrP^{Sc}, and unfolding curves obtained with mAb 12B2 report on the unfolding of type 1 only, we constructed differential curves of the stability of rPrP^{Sc} for each sCJD case. These differential unfolding curves of rPrP^{Sc} correspond to the stability profiles of type 2 rPrP^{Sc} (Fig. 2*F*).

Cumulatively, CDI data demonstrate two populations of conformers with distinctly different stabilities and responses to PK treatment. The stabilities of type 2 rPrP^{Sc} co-occurring in the same sCJD host and in the same location are invariably lower after the PK treatment than the stability of type 1 rPrP^{Sc}. These findings are in accord with our previous observations demonstrating the lower stability of undigested oligomers of type 1 sCJD PrP^{Sc} than type 2 sCJD PrP^{Sc} and opposite effects of PK treatments leading to the lower stability of residual pure type 2 sCJD rPrP^{Sc} and the higher stability of residual pure type 1 rPrP^{Sc} (15, 16).

Prion Particle Size and Composition in sCJD Cases with Mixed Type 1 + 2 PrP^{Sc}—To investigate sCJD prion particle size and composition, we separated the prion particles according to sedimentation velocity using high speed centrifugation in sucrose gradient. The sCJD prions present in the brain homogenates of six sCJD patients with mixed type 1 + 2 PrP^{Sc} in the same location were separated in 10–45% sucrose gradients, and the collected fractions were analyzed before and after PK treatment by WBs and CDI. WBs of the fractions developed with mAb 12B2 specific for type 1 rPrP^{Sc} (17, 20) and mAb 1E4 preferential for type 2 rPrP^{Sc} (20) indicate that most of the PrP^{Sc} collected in fractions 3–5 were composed of type 1 rPrP^{Sc} (Fig. 3, *A* and *B*). In contrast, type 2 was present predominantly in fraction 1 in all six cases examined (Fig. 3, *A* and *B*). The PrP^{Sc} present in pure type 1 sCJD brain homogenate, and mixed *in vitro* with type 2 sCJD brain homogenate, separated in a similar manner; type 1 was collected in fractions 3–5, and type 2 sedimented mostly to fraction 1 (Fig. 3, *C* and *D*).

Next, we performed a CDI using sucrose gradient fractions obtained from six mixed type 1 + 2 cases. The parallel CDI conducted with mAb 3F4 (Fig. 4*A*) and with mAb 12B2 (Fig. 4*B*) allowed for the measurement of different PrP^{Sc} isoforms, type 1 rPrP^{Sc} directly and type 2 rPrP^{Sc} by subtracting the concentration of type 1 rPrP^{Sc} from total rPrP^{Sc}. The results expressed as a relative fractional distribution (F_{app}) confirmed the data obtained with WBs and showed that the maximum level of type 1 rPrP^{Sc} was present in fractions 3–5, whereas type 2 sedimented to the bottom of the tube (Fig. 4*C*). We concluded from these experiments that co-existent type 1 + 2

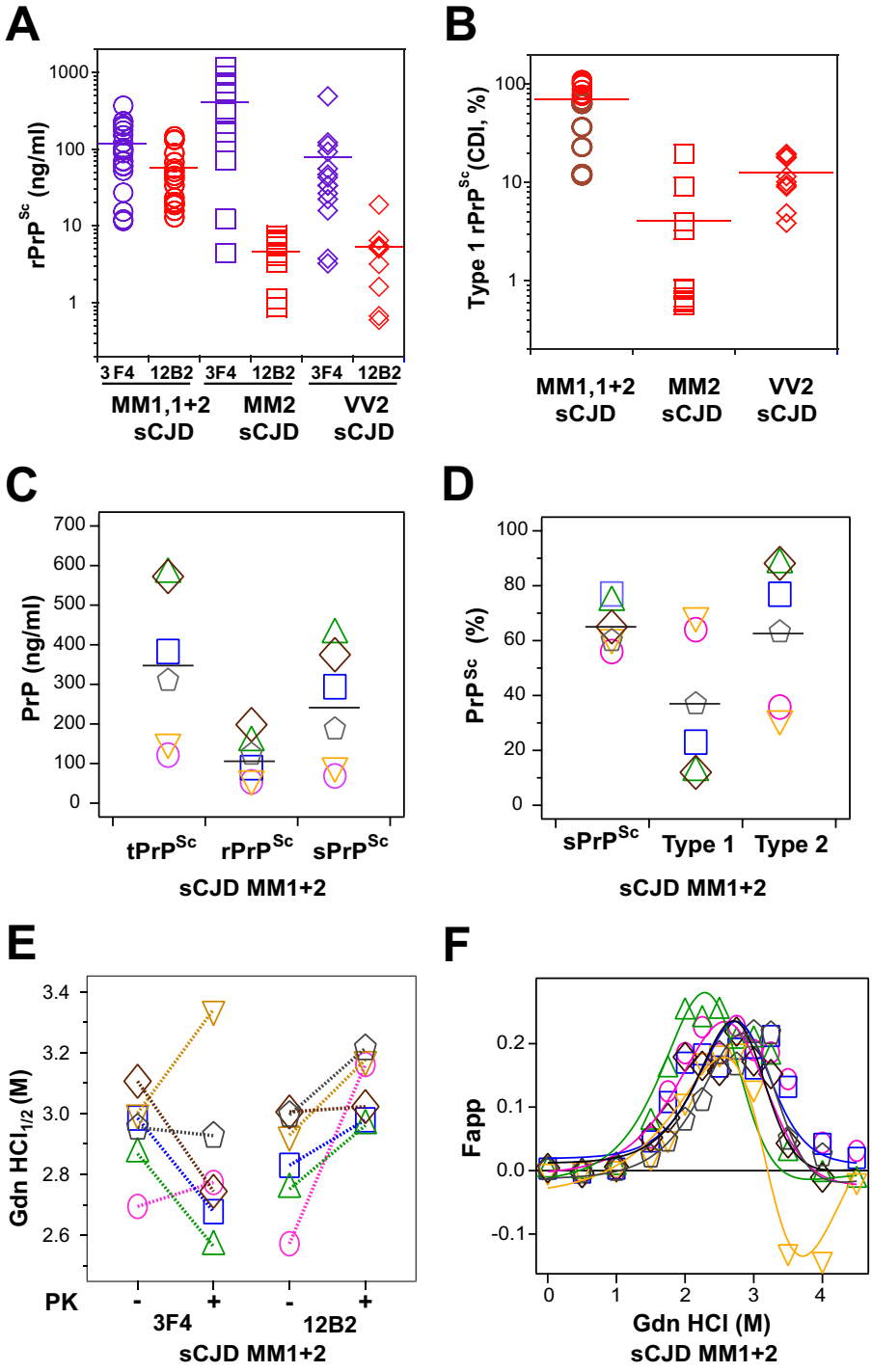

FIGURE 2. **Concentration and dichotomous impact of PK treatment on the conformational stability of PrP^{Sc} isoforms in the cortex of sCJD with mixed type 1 + 2 PrP^{Sc} in the same location.** *A*, concentration of total and type 1 rPrP^{Sc} in the cortex of 36 cases of sCJD homozygous for different codon 129 polymorphisms and with WB classification of MM type 1 ($n = 10$), MM type 2 ($n = 10$), VV type 2 ($n = 10$), and MM type 1 + 2 ($n = 6$) rPrP^{Sc} in the same location. *B*, relative proportion of type 1 rPrP^{Sc} in each codon 129 polymorphism and WB classification group; the sCJD cases MM type 1 + 2 ($n = 6$) studied in detail in this paper are depicted as *brown circles*. *C*, concentrations of total PrP^{Sc} (*purple circles*), rPrP^{Sc} (*black circles*), sPrP^{Sc} (*green diamonds*). *D*, relative proportion of sPrP^{Sc} (*green diamonds*), type 1 (*red triangles*), and type 2 (*blue triangles*) in each sCJD case ($n = 6$). *E*, distinct conformational stability of total rPrP^{Sc}, type 1 rPrP^{Sc}, and incongruent impact of proteinase K treatment (−/+). The same color symbols and links indicate data obtained in the same mixed case of sCJD. *F*, differential stability curves of type 2 rPrP^{Sc} obtained after subtracting stability curves of type 1 rPrP^{Sc} obtained with mAb 12B2 from stability curves of total rPrP^{Sc} obtained with mAb 3F4 after PK treatment. The CDI with europium-labeled mAb 3F4 was used to determine the concentration and stability of total PrP^{Sc} and mAb 12B2 to measure the concentration and stability of type 1 rPrP^{Sc}. Each data *point* represents a unique patient measured in triplicate, and the concentration of PrP^{Sc} in 10% brain homogenate was calculated; the percentage of rPrP^{Sc} or type 1 is expressed over total rPrP^{Sc}. The *horizontal line* represents mean for each parameter.

PrP^{Sc} is composed of a mixture of distinct type 1 and type 2 particles, which can be separated according to their different sedimentation velocities. Additionally, the mixing of both PrP^{Sc} types *in vitro* did not induce changes in sedimentation that would indicate an interaction of type 1 and type 2 PrP^{Sc} particles.

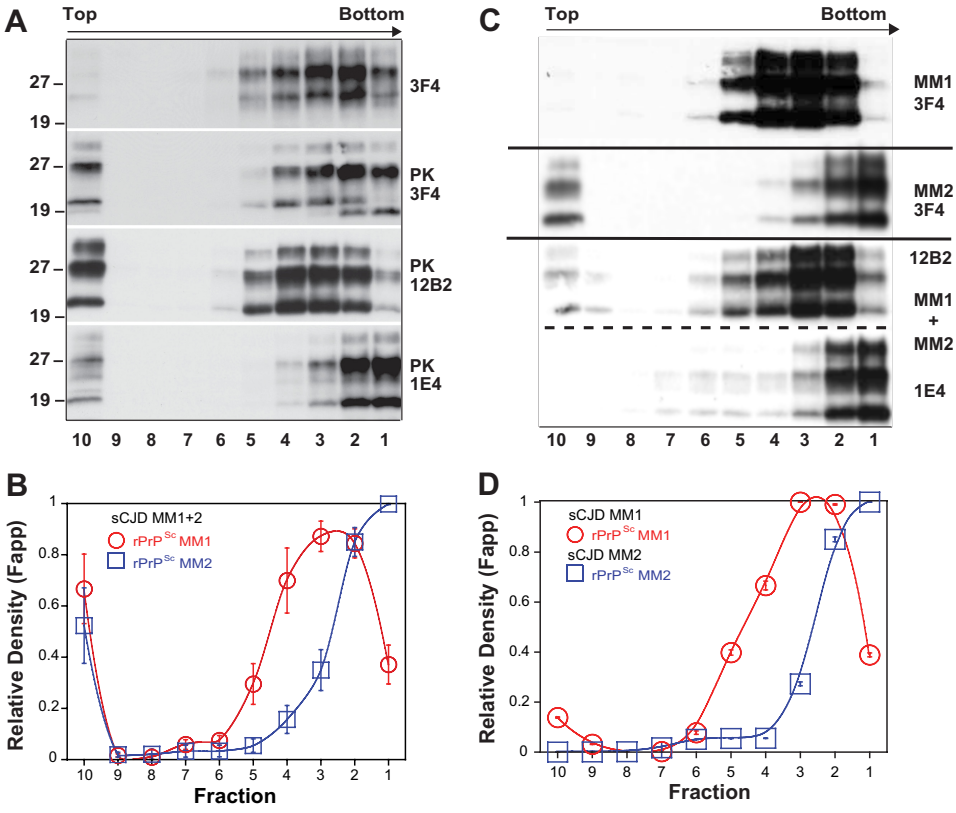

FIGURE 3. **Mixed type 1 + 2 sCJD PrP^{Sc} present in the same cortical location of sCJD separated by sedimentation velocity fractionation in sucrose gradient into type 1 and type 2 sCJD PrP^{Sc}.** *A*, representative distribution of total PrP^{Sc} before or after PK was monitored with mAb 3F4, type 1 with mAb 12B2, and type 2 with mAb 1E4 after PK in a typical mixed type 1 + 2 case of sCJD. *B*, cumulative plot of relative distribution of type 1 (*red circles*) and type 2 rPrP^{Sc} (*blue squares*) in sucrose gradients of six sCJD patients with mixed type 1 + 2 PrP^{Sc} present in the same cortical location. *C*, representative distribution of type 1 rPrP^{Sc} of a typical pure MM1 sCJD, pure type 2 rPrP^{Sc} in typical MM2 sCJD, and after mixing both types before in sucrose gradient. *D*, relative distribution of type 1 (*red circles*) and type 2 rPrP^{Sc} (*blue squares*) in sucrose gradient after densitometry of WBs shown in *C*. The total PrPs were monitored with mAb 3F4, type 1 with mAb 12B2, and type 2 with mAb 1E4 after PK. The Western blots were developed before or after PK digestion was performed with 3 IU/ml (~100 μg/ml) of 10% brain homogenate for 1 h at 37 °C and scanned using ImageJ. The data points are mean ± S.E. from six sCJD cases each scanned in triplicate.

Conformational Stability of Mixed Type 1 + 2 PrP^{Sc} Fractionated in Sucrose Gradient—The conformational stability of rPrP^{Sc} collected from mixed type 1 + 2 cases in fraction 4 of the sucrose gradient was markedly different from the stability obtained in fraction 1 (Fig. 4*D*). The stability of rPrP^{Sc} collected in fraction 4 and fraction 1 was similar to the stability of type 1 PrP^{Sc} and type 2 PrP^{Sc}, respectively, collected from pure MM1 or MM2 cases of sCJD (Fig. 4*E*). Mixing brain homogenates of pure type 1 and type 2 sCJD *in vitro* did not change the sedimentation velocity of rPrP^{Sc}, and the stability of each type of rPrP^{Sc} remained unchanged. We concluded that brain homogenates of mixed type 1 + 2 sCJD contain particles of different sizes in the same cortical location, with distinctly different stabilities, corresponding in general to the range we have seen in pure type 1 or pure type 2 sCJD, as observed previously after PK treatment (15, 16). The experiments also confirmed our earlier observation of a paradoxically decreased stability of type 2 sCJD PrPSc after PK treatment (15). The mixing experiments performed *in vitro* did not indicate any interaction between type 1 and type 2 particles or the formation of hybrid aggregates.

PMCA of Mixed Type 1 + 2 sCJD PrP^{Sc}—In the next experiments, we addressed the question whether the type 1 and type 2 particles in the mixture replicate independently as would be expected from a mixture of different prions. The WBs performed on the reaction product generated in sPMCA with homologous human PrP^{C} substrate expressed in the brains of Tg(HuPrP,129M) mice (15, 50) were developed with mAb 3F4 to detect total rPrP^{Sc}, and with mAb 12B2 for type 1 rPrP^{Sc} (Fig. 5, *A–C*). The impact of amplification on the type 1 and type 2 doublet was difficult to investigate directly due to the limited amplification rate and low concentrations of unglycosylated PrP^{Sc} in the reaction product. The enzymatic deglycosylation revealed a sudden change in the reaction product with a dominant band of type 1 and absent type 2 PrP^{Sc} (Fig. 5*C*). The second band with an apparent mass of ~27 kDa corresponds to the deglycosylated PrP^{Sc} that remained incompletely digested even after 1 h of incubation with up to 100 μg/ml of PK at 37 °C in the presence of 1% Sarkosyl; this highly PK-resistant subfraction was observed after PMCA by us and others previously (11, 15). To investigate the abrupt transition in detail and to "slow down" the conformational transformation of PrP^{Sc} from original human brain homogenate seed, we decided to use only a 2-fold dilution between sequential PMCA rounds, in contrast to the usual 10-fold dilution of the reaction product, into fresh substrate Tg(HuPrP) brain homogenate. The WB data confirmed previous observations (Fig. 6, *A* and *B*) and show preferential amplification of type 1 over type 2 rPrP^{Sc}; the same trends were observed in the experiments followed with CDI (Fig. 6, *C–E*). These data indicate that mixed sCJD cases are composed of two distinct populations of conformers that rep-

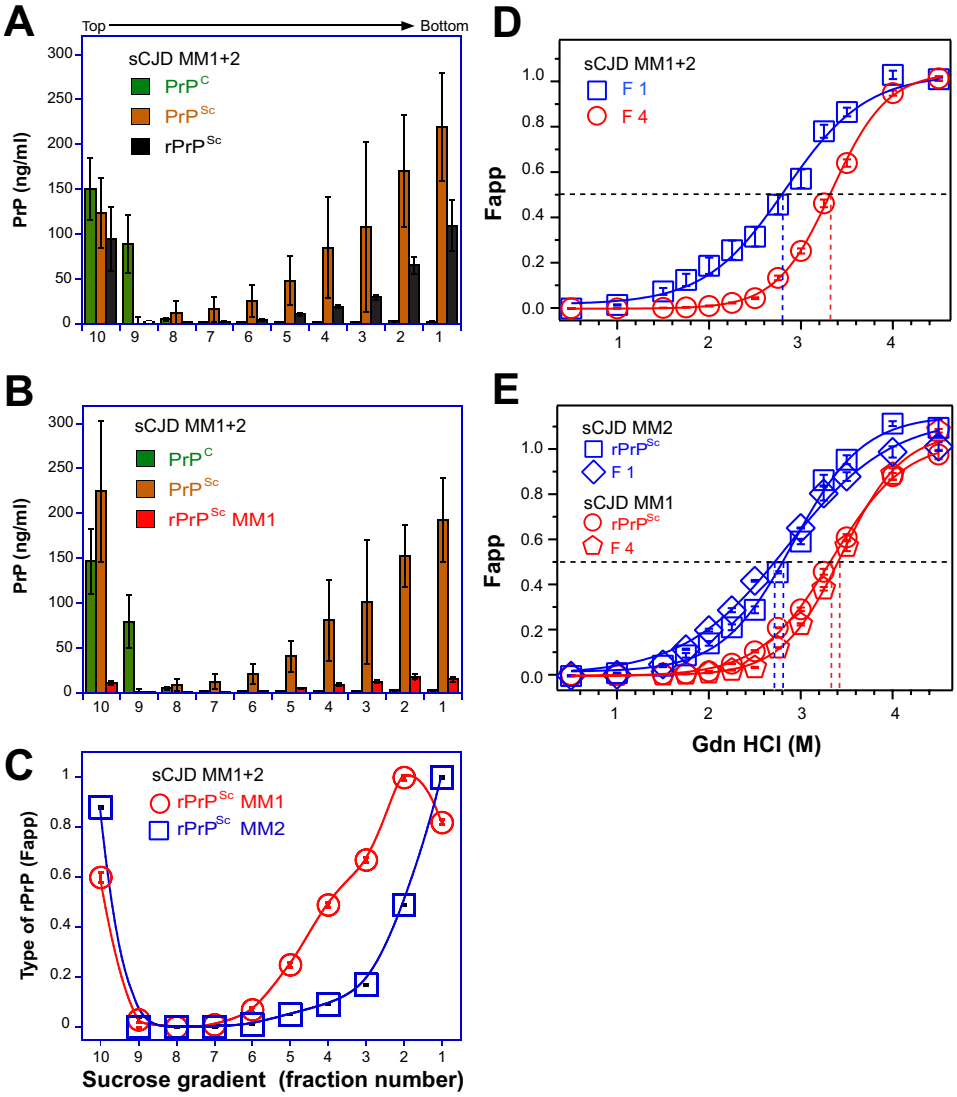

FIGURE 4. **Sedimentation velocity fractionation and conformational stability of PrPs monitored with CDI in sCJD cases with mixed type 1 + 2 rPrP^{Sc}.** *A*, concentrations of PrP^{C} (*green bars*), total PrP^{Sc} (*brown bars*), and rPrP^{Sc} (*black bars*) determined with europium-labeled mAb 3F4. *B*, concentration of type 1 rPrP^{Sc} (*red bars*), PrP^{C} (*green bars*), and total PrP^{Sc} (*brown bars*) determined with europium-labeled mAb 12B2. *C*, relative proportion of type 1 (*red circles*) and type 2 (*blue squares*) rPrP^{Sc}. *D*, representative conformational stability curve of type 1 rPrP^{Sc} obtained in fraction 4 (*red circles*) and type 2 rPrP^{Sc} (*blue squares*) obtained in fraction 1 of the sucrose gradient of mixed type 1 + 2 sCJD. *E*, typical conformational stability curves of pure type 1 rPrP^{Sc} of MM1 sCJD and type 2 rPrP^{Sc} of MM2 sCJD that were mixed *in vitro*. The original MM1 sCJD rPrP^{Sc} before (*red circles*) and fraction 4 after mixing and sucrose gradient separation (*red pentagons*) are shown; the original MM2 sCJD rPrP^{Sc} before (*blue squares*) and fraction 1 after mixing and sucrose gradient separation (*blue diamonds*) are shown. The fractions were obtained from the frontal ($n = 3$) or occipital ($n = 3$) cortex of six mixed type 1 + 2 sCJD cases. The total rPrP^{Sc} was measured with europium-labeled mAb 3F4, type 1, with europium-labeled mAb 12B2, and the difference is type 2 rPrP^{Sc}. The *bars* and *data points* are an average ± S.E. obtained in six cases each measured in triplicate with CDI before and after PK treatment as described in the legend for Fig. 3.

licate in PMCA independently, with preferential amplification of the type 1 PrP^{Sc} particles. The data extend our previous observations of generally more efficient amplification of type 1 PrP^{Sc} due to the lower conformational stability (15, 16).

To investigate the impact of an alternative substrate on the amplification of mixed type 1 and type 2 PrP^{Sc} particles and the adaptation process, we introduced as a substrate brain homogenates from transgenics that express unglycosylated PrP^{C} (Tg(HuPrP^{N181Q,N197Q},129M)). Even though the PrP^{C} levels in the Tg(HuPrP^{N181,197Q},129M) are 60% of the level in FVB mice (Fig. 6, *A* and *B*), this substrate amplifies both pure type 1 and type 2 PrP^{Sc} and offers the critical advantage of an unequivocal high intensity band of unglycosylated PrP^{Sc} without enzymatic deglycosylation. The WBs performed on the reaction product generated in nine rounds of sPMCA were developed with mAb 3F4 to detect total rPrP^{Sc}, with mAb 12B2 for type 1 rPrP^{Sc} and mAb 1E4 for type 2 rPrP^{Sc} (Fig. 7*A*). The WBs indicate a gradual loss of type 2 rPrP^{Sc} bands from the original doublet in the mixed type 1 + 2 sCJD samples, and after an adaptation period in rounds 4–6, the dominant band became type 1 rPrP^{Sc}. The experiments performed with pure type 1 sCJD (Fig. 8*A*) or pure type 2 sCJD (Fig. 8*B*) show within nine rounds of sPMCA a faithful replication of the unglycosylated rPrP^{Sc} from the original sCJD brain homogenate.

The sPMCA of mixed type 1 + 2 sCJD cases was also followed by CDI. We used europium-labeled mAb 3F4 for the detection of total rPrP^{Sc} and europium-labeled mAb 12B2 for the selective detection of type 1 rPrP^{Sc} (Fig. 7*B*). The amplifica-

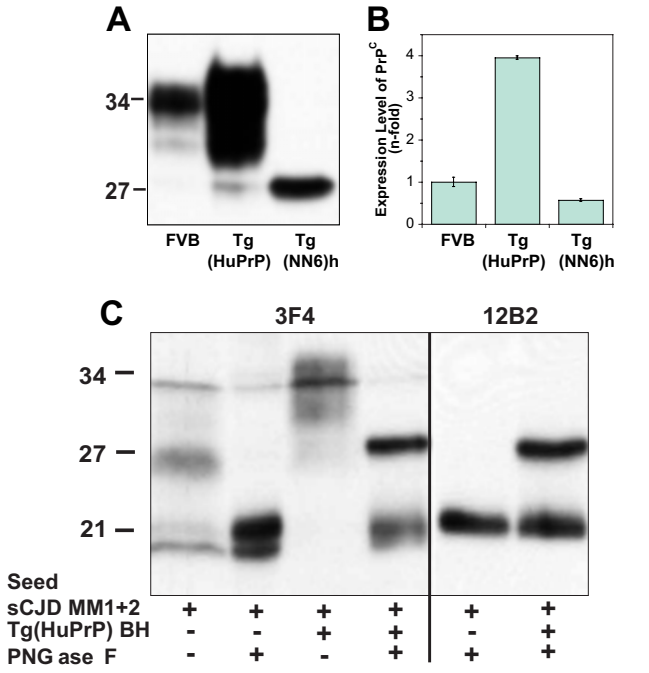

FIGURE 5. **Expression levels of PrP^{C} in Tg(HuPrP) and Tg(NN6)h mice and sPMCA of sCJD MM1 + 2 PrP^{Sc} with human PrP^{C} substrate.** *A,* Western blot pattern and levels of PrP^{C} and nonglycosylated PrP$^{C(N181Q/N197Q)}$ in the brain homogenate of Tg(HuPrP) and Tg(NN6)h mice, respectively, developed with mAb 12B2. *B,* relative expression levels of PrP^{C} and PrP$^{C(N181Q/N197Q)}$ in Tg(HuPrP) and in Tg(NN6)h mouse brains, respectively, were measured with europium-labeled mAb 12B2 by CDI and compared with the levels in FVB mice. *C,* preferential amplification of type 1 PrP^{Sc} in sPMCA of mixed type 1 + 2 cases using Tg(HuPrP) and followed by WBs. The sPMCA was performed with homologous human PrP^{C} as described previously (15) and 10-fold dilution of type 1 + 2 sCJD brain homogenate. The reaction product was after sPMCA and PK treatment deglycosylated with peptide:*N*-glycosidase F (*PNGase F*).

tion index was calculated in each round using the following: (PMCA rPrP^{Sc})/((seed rPrP^{Sc})/2^{n}), taking into account the number (n) of PMCA rounds and sequential 2-fold dilution of the seed between rounds. The regression analysis of amplification indexes obtained with six mixed sCJD cases after nine rounds of PMCA indicated consistently higher amplification rates of the type 1 rPrP^{Sc} in comparison with the total rPrP^{Sc} (Fig. 7*B*). To understand the dynamics of changes and inter-individual differences, we performed new experiments with sequential CDI after each round and with both antibodies. The control experiments with pure type 1 and type 2 sCJD replicated both rPrP^{Sc} conformers efficiently, with type 2 replicating faster and with a less prominent adaptation phase (Fig. 7, *C* and *D*). Even though the amplification index varied significantly between different cases of mixed type 1 + 2 sCJD, the data obtained with mAb 12B2 are in agreement with the data obtained using mAb 3F4, which indicate that the primary amplifying species from the mixture was type 1 rPrP^{Sc} (Fig. 7, *E* and *F*). Thus, the more sensitive and specific CDI confirmed qualitative WB findings, and both methods support the conclusion that type 1 conformers present in a mixture of type 1 + 2 rPrP^{Sc} replicate independently and more efficiently and as a result dominate the later rounds of sPMCA. In contrast, the type 2 conformers initially present in the mixture gradually disappeared. This adaptation phase, which apparently differs between different sCJD PrP^{Sc}, is intriguing and may suggest distinct optimum PrP^{Sc}/PrPC stoichiometry for the conversion of different PrP^{Sc} conformers or an adaptation to different auxiliary molecules that may be species-specific.

The conformational stability assay of rPrP^{Sc} performed with CDI using mAb 12B2 showed a dramatic shift of type 1 rPrPSc to the less stable conformers after nine rounds of PMCA with unglycosylated PrP$^{C(N181,197Q)}$ substrate (Fig. 9*A*). In control experiments performed with pure type 2 sCJD, the unfolding curves of rPrP^{Sc} collected before and after PMCA were superimposable (Fig. 9*B*). These experiments indicate that PMCA performed with unglycosylated PrP$^{C(N181,197Q)}$ substrate and sCJD PrP^{Sc} harboring predominantly type 1 or type 2 propagate these conformers with high fidelity. The data are in accord with our previous observations showing that the faster replication of type 1 PrP^{Sc} *in vitro* is due to the higher proportion of less stable protease-sensitive oligomers than in type 2 PrP^{Sc} (5, 15). Consequently, in "mixed" cases of sCJD, type 1 rPrP^{Sc} replicated preferentially, and its stability significantly decreased further below the stability of type 1 that was observed in the original brain homogenate. Cumulatively, these data indicate that mixed sCJD cases are composed of two populations of conformers that replicate in PMCA independently and, under favorable conditions, may undergo further conformational selection in favor of faster replicating, less stable conformers.

DISCUSSION

Here, we disclose two major phenomena defining sporadic human prion diseases as follows: (*a*) the co-existence of two distinct populations of human PrP^{Sc} particles in the same host; and (*b*) a conformational evolution of human PrP^{Sc} by natural selection. Using sedimentation velocity separation by high speed centrifugation in sucrose gradient, we show that PrP^{Sc} in mixed type 1 + 2 sCJD is a blend of distinct type 1 and type 2 particles, each composed of conformers with unique stability and replication rates *in vitro*. Each of these features offer evidence of a distinct prion strain and suggest that distinct prions frequently co-exist in the most prevalent human prion disease, sCJD. Remarkably, the independent replication of type 1 PrP^{Sc} with novel PrP^{C} substrate leads to gradual evolution by natural selection of the conformational subset with the highest replication rate due to the lowest stability.

Co-existence of Distinct PrP^{Sc} Conformers in sCJD—Our CDI data obtained with mAb 12B2 (Fig. 2, *A* and *B*) are in accord with WB observations obtained with more sensitive and specific antibodies that uncovered frequent, and probably ubiquitous, co-existence of 21-kDa (type 1) and 19-kDa (type 2) fragments of unglycosylated rPrP^{Sc} in the same human prion-infected brain (17–21). Additionally, the growing body of evidence accumulated with sensitive conformational methods, including CDI, indicates extensive conformational heterogeneity of sCJD rPrP^{Sc} fragments that otherwise show a single band (type) on WBs (5, 15–17). Thus, the remarkably variable phenotypes of all human prion diseases, including sporadic CJD, apparently stems from the *PRNP* gene polymorphisms in codon 129 of the *PRNP* gene and a complex interaction with different conformers of PrP^{Sc} (5, 6, 14, 22). Taken together, the pure type

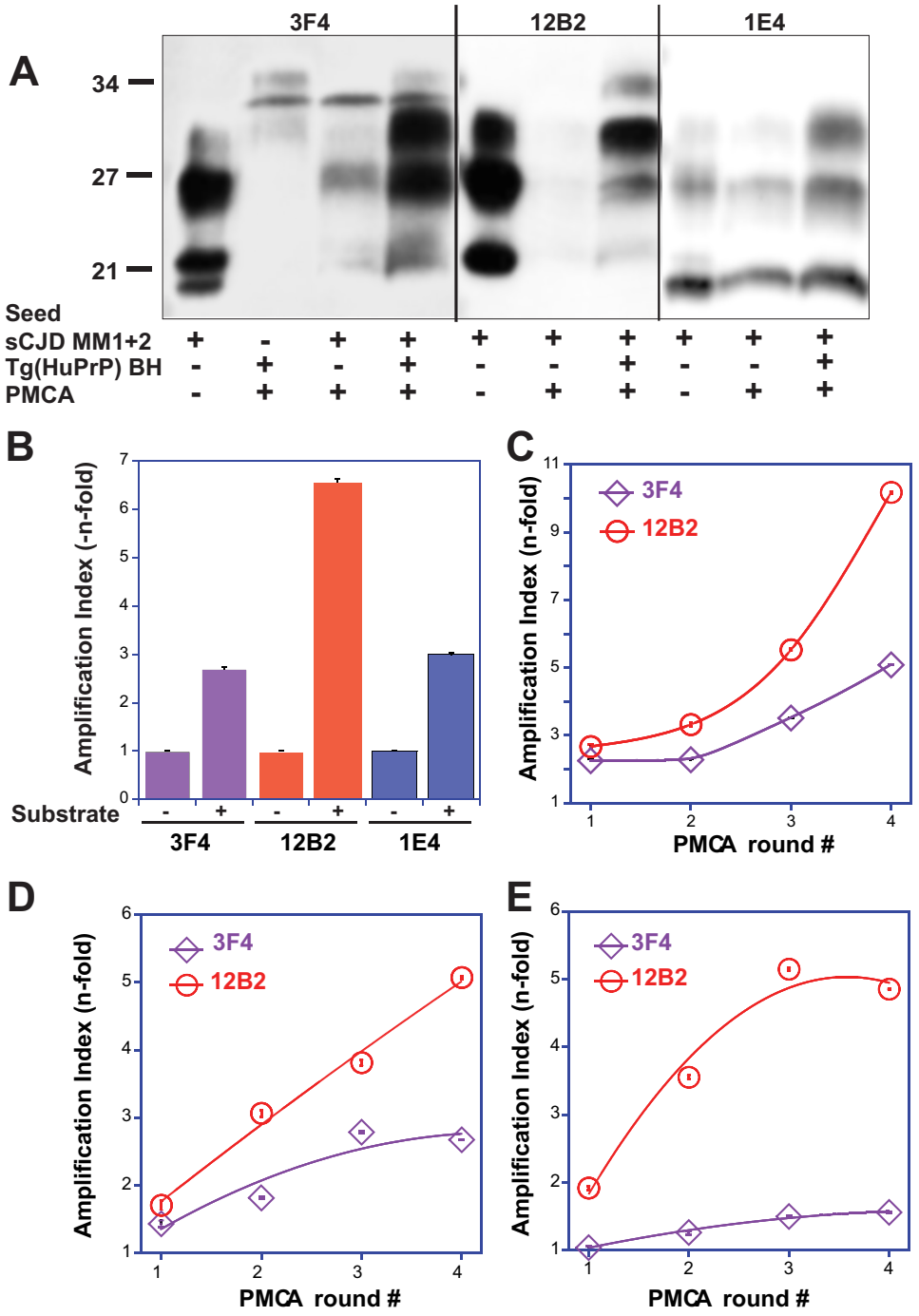

FIGURE 6. **Preferential amplification of type 1 PrP^{Sc} in sPMCA of mixed type 1 + 2 cases followed by WBs and CDI.** The sPMCA was performed with homologous human PrP^{C} as described previously (15) with limited 2-fold dilution between rounds. *A*, representative WB was developed with mAb 3F4 for both type 1 and type 2, mAb 12B2 for type 1, and mAb 1E4 for type 2 PrP^{Sc}. *B*, amplification index of different types of PrP^{Sc} followed by WB densitometry. *C–E*, amplifications of different mixed cases with type 1 + 2 PrP^{Sc} in sPMCA followed by CDI with europium-labeled mAb 3F4 for total PrP$_{Sc}$ (*purple diamonds*) and 12B2 selective for type 1 PrP^{Sc} (*red circles*) and expressed as an amplification index.

1 or type 2 cases may frequently contain low levels of the second minor component (type 2 or type 1, respectively), which is not detected by regular WBs.

We used the measurement of sedimentation velocity (51) to investigate whether co-existent type 1 and type 2 rPrP^{Sc} form distinct particles in the brains of patients with mixed type 1 + 2 sCJD in the same cortical location. We previously observed a broad range of sedimentation velocities using ultracentrifugation of sCJD brain homogenates in sucrose gradient, which indicates that sCJD PrP^{Sc} proteins exist in the continuum of aggregates composed from <20 to >600 PrP^{Sc} molecules (15). However, the major fraction of type 2 rPrP^{Sc} conformers showed strikingly high sedimentation velocity, in contrast to the lower sedimentation velocity of MM1 PrP^{Sc}, indicating that type 2 PrP^{Sc} formed aggregates with different sizes, shapes, or both (15). We used the differences in sedimentation velocity here to isolate type 1 and type 2 rPrP^{Sc} from the mixture extracted from sCJD brains and to characterize them confor-

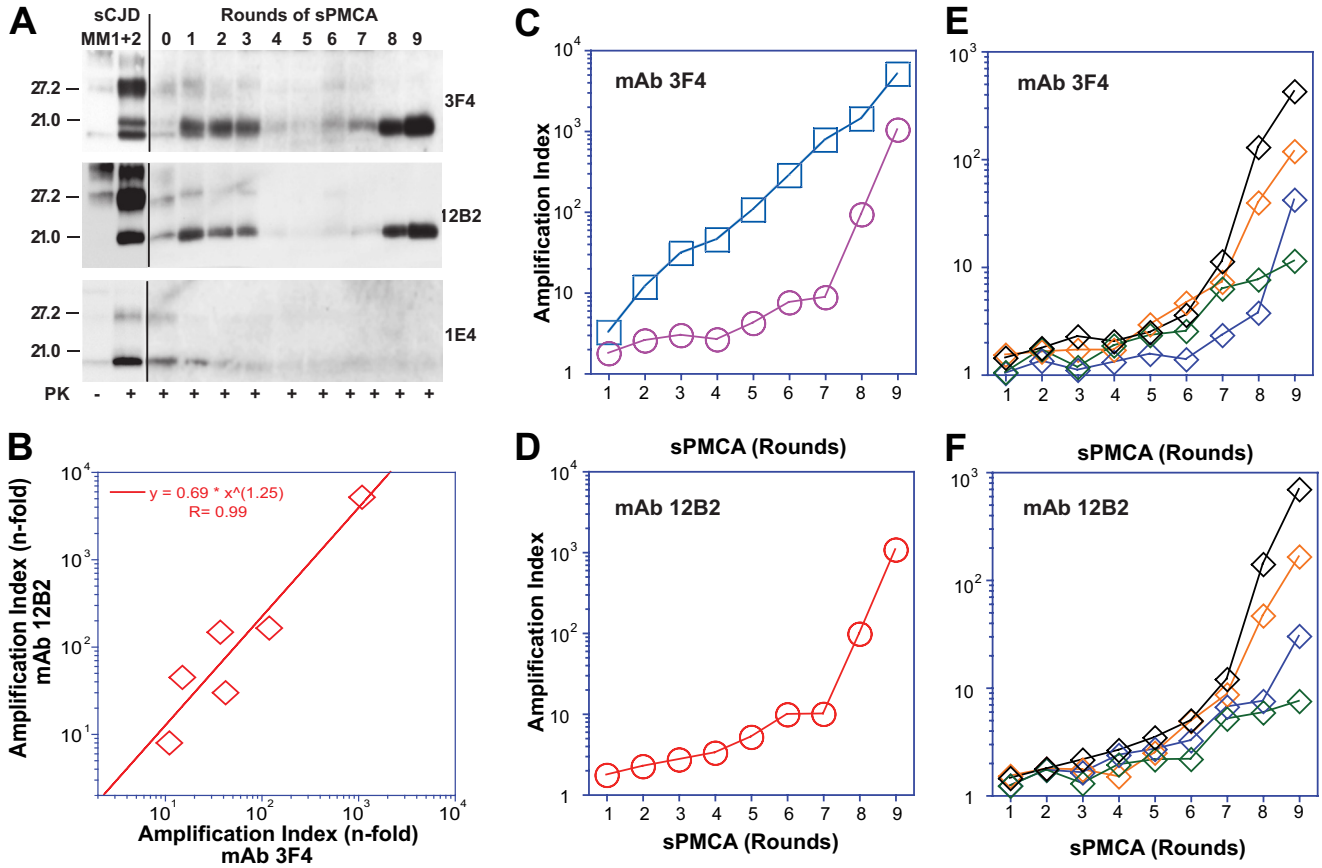

FIGURE 7. **PMCA of mixed type 1 + 2 PrP^{Sc} with PrP$^{C(N181Q,N197Q)}$ substrate.** The sPMCA was performed with initial 10-fold dilution of type 1 + 2 sCJD brain homogenate followed by limited 2-fold dilution between rounds. *A,* representative WB was developed with mAb 3F4 for both type 1 and type 2, mAb 12B2 for type 1, and mAb 1E4 for type 2 PrP^{Sc}. *B,* amplification index of total PrP^{Sc} and type 1 PrP^{Sc} was determined with CDI in six cases of type 1 + 2 sCJD using europium-labeled mAb 3F4 and europium-labeled mAb 12B2, respectively, after 9 rounds of PMCA. *C* and *D,* amplification of pure type 1 (*red circles*) PrP^{Sc} and pure type 2 (*blue squares*) in sPMCA followed by CDI with europium-labeled mAb (*C*) 3F4 or (*D*) 12B2 and expressed as an amplification index. *E* and *F,* amplification indexes of mixed cases of type 1 + 2 sCJD (*diamonds*) followed with mAb 3F4 (*E*) or 12B2 (*F*).

mationally. The data indicate that type 1 and type 2 rPrP^{Sc} co-existing in the same cortical location form distinct particles, which are composed of homogeneous populations of conformers that have uniform N-terminal proteolytic cleavage sites and conformational stability. Because both types of particles had Gaussian distribution and overlapped in some fractions, we asked whether a minor fraction of these conformers may interact or form hybrid particles. This is apparently not the case, because we observed no changes in the sedimentation velocity of aggregates nor any formation of hybrids after mixing different types *in vitro*. Taken together with the growing number of independent studies indicating that type 1 and type 2 rPrP^{Sc} co-exist in high proportion, and likely in the majority of sCJD cases, our findings suggest that the co-existence of distinct prion particles is a common feature of sCJD. The different quaternary structure, or packing of the monomers of PrP^{Sc} with different conformations in distinct particles, is responsible for the peptide fragmentation pattern, consisting of predominantly 19-kDa fragments in type 2 rPrP^{Sc} or 21 kDa in type 1 rPrP^{Sc}, after PK treatment.

Implications for Adaptation, Competition, Evolution, and Selection of Prions—Although the possible co-existence of different prions in naturally prion-infected sheep, goat, and mink has been suspected early on (7, 52–56), these experiments could not discriminate between two possibilities as follows: (*a*) selection of strains from a co-existing pool in the natural host, or (*b*) strain adaptation (mutation) caused by the switch from the primary sequence of the original host's PrP^{Sc} to the different PrP sequence in the new host (57, 58). We used a modified PMCA with homologous as well as unglycosylated PrP$^{C(N181Q,N197Q)}$ substrate to test whether the type 1 and type 2 particles of PrP^{Sc} we isolated in sucrose gradients replicate independently as is expected for different prions (46). The unglycosylated PrP$^{C(N181Q,N197Q)}$ expressed in the brains of transgenic mice that carry the PrP construct with double N181Q and N197Q mutations, allowed for direct monitoring of unglycosylated bands of type 1 and type 2 rPrP^{Sc} in PMCA with WBs, and thus the detection of subtle changes in their mobility and ratio without additional enzymatic deglycosylation.

In contrast to pure type 2 sCJD seeds, the serial PMCA of pure type 1 and mixed type 1 + 2 seeds underwent two distinct phases. In the first adaptation phase, the amplification was limited, and as a result, the bands of unglycosylated rPrP^{Sc} gradually disappeared on WBs; the amplification was detectable only with CDI. In the second phase, we observed an abrupt increase in the amplification rate from 64- to 128-fold dilution of the original seed in rounds 6 and 7. Within the type 1 + 2 mixture, type 2 rPrP^{Sc} gradually disappeared, even though pure type 2

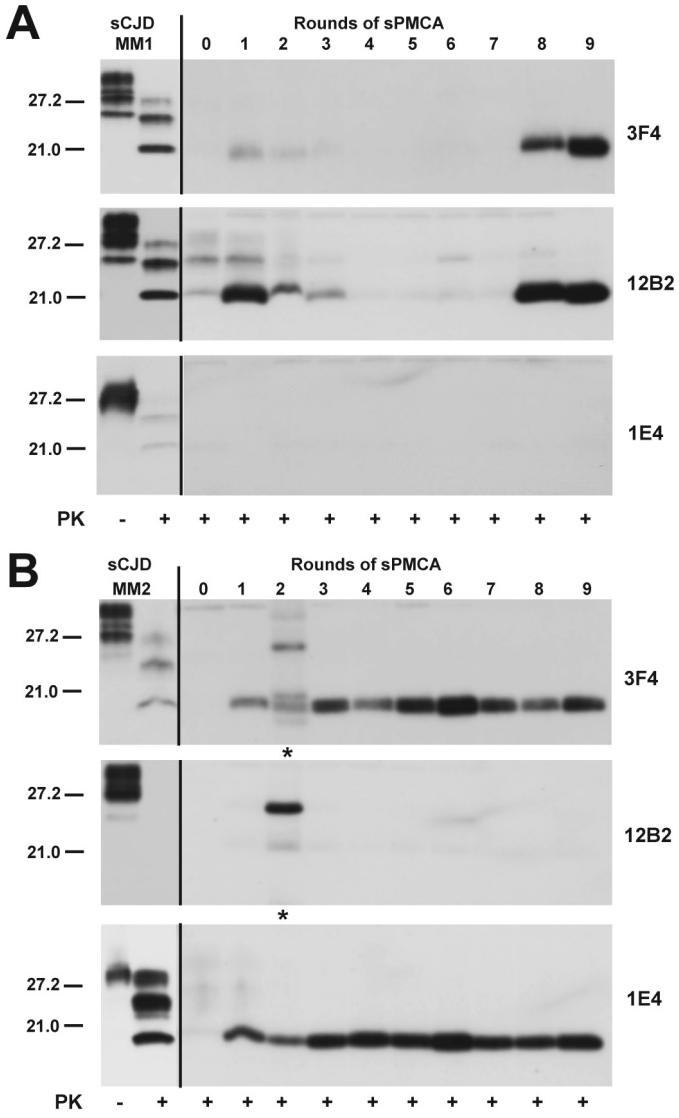

FIGURE 8. **Selective amplification of pure type 1 or pure type 2 sCJD PrP^{Sc} using PrP$^{C(N181Q/N197Q)}$ substrate.** The sPMCA was performed as described with initial 10-fold dilution of pure sCJD type 1 (*A*) and pure type 2 sCJD(*B*). The total rPrP^{Sc} was after PK treatment detected with mAb 3F4, type 1 rPrP^{Sc} with mAb 12B2, and type 2 with mAb 1E4. The incompletely PK-digested PrP^{Sc} in *B* is indicated by an *asterisk*.

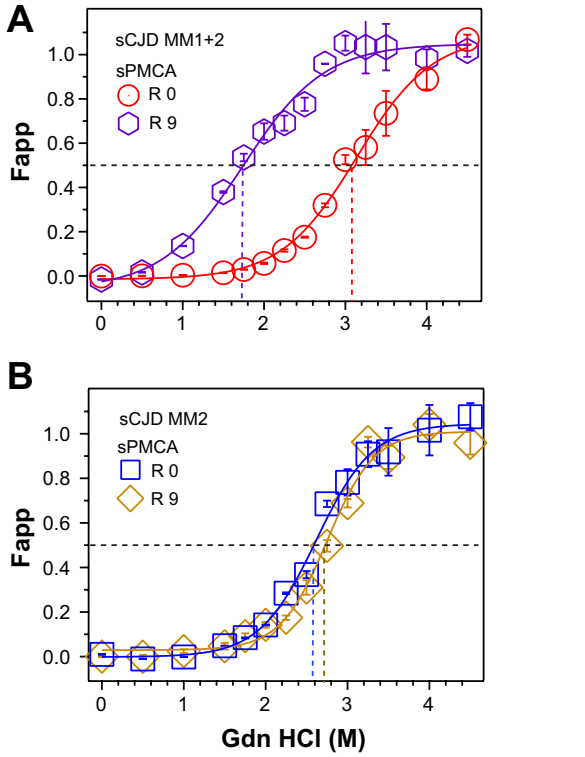

FIGURE 9. **Selection of type 1 rPrP^{Sc} and further shift in conformational stability after PMCA of mixed type 1 + 2 sCJD with unglycosylated PrP^{C} substrate.** *A*, conformational stability curve of type 1 rPrP^{Sc} obtained with europium-labeled mAb 12B2 before (*red circles*) and after 9 rounds of PMCA (*purple hexagons*). *B*, conformational stability curve of a typical pure type 2 rPrP^{Sc} obtained with europium-labeled mAb 3F4 before (*blue squares*) and after 9 rounds of PMCA (*yellow diamonds*).

sCJD amplified very well. This resulted in the uniform selection of type 1 rPrP^{Sc} in mixed type 1 + 2 cases (Fig. 7, *A* and *B*). Surprisingly, even though the N-terminal PK cleavage sites and mobility on WBs corresponded to the type 1 rPrP^{Sc} from the original brain type 1 + 2 mixture, the stability of the PMCA rPrP^{Sc} significantly dropped in comparison (Fig. 9, *A* and *B*). These findings provide experimental evidence for an evolutionary process within the type 1 + 2 mixture, with selection that favors type 1 conformers with the lowest stability. The initial preferential amplification rate of type 1 PrP^{Sc} is not surprising due to the usually higher percentage of less stable protease-sensitive oligomers and may explain the predominant presence of type 1 PrP^{Sc} in ~70% of all sCJD cases (5, 15). These data correlate with the superior transmissibility and short incubation times of MM1 sCJD prions and with incomplete transmissions and extended incubations times of MM2 sCJD prions observed in transgenic mice overexpressing homologous or chimeric human PrP^{C} (59, 60). Moreover, the dramatic difference in the amplification rate of pure type 2 compared with type 2 present in the type 1 + 2 mixture suggests an interference between type 1 and type 2 conformers. The prion interference has been observed *in vivo* in mice (61) and Syrian hamsters (62) that were inoculated simultaneously or sequentially with two distinct strains of prions. The exact molecular mechanism of this phenomenon remains to be fully elucidated, but because we observed no direct interaction between different conformers of PrP^{Sc}, the most likely explanation is a competition for PrP^{C} substrate or auxiliary molecule implied from experiments with Syrian hamster-adapted prions (63).

Cumulatively, the distinct particle size, conformational stability, and amplification rate all argue for the frequent co-existence of different sCJD prions in the same host. Under favorable conditions with compatible PrP^{C} substrate, the mixture of human PrP^{Sc} conformers may undergo an evolution that selects a subset with the highest replication rate, due to their lowest stability. Notably, the adaptation phase and prion strain evolution inferred from experiments with clone cells (10) and Tg mice (57, 58), has been shown here to be a conformational process. It remains to be established, however, whether the first adaptation phase is due to the requirement for the critical threshold stoichiometry of PrP^{Sc}/PrP$^{C(N181Q,N197Q)}$ needed for optimum replication (adaptation due to the absence of sugar

chains on PrP$^{C(N181Q,N197Q)}$ substrate and double Asn to Gln mutation) or whether this first phase is caused by the difference between mouse and human auxiliary molecules. Even though the enzymatic deglycosylation had no impact on the biological characteristics of prions replicated in PMCA (64), and the conservative Asn to Gln mutations are outside the central PrP region between residues 96 and 167, which has a major role in determining the species barrier (57, 58), the evaluation of biological characteristics of nonglycosylated sCJD prions generated with PrP$^{C(N181Q,N197Q)}$ must await the results of ongoing bioassays.

Concluding Remarks and New Directions—Several explanations have been proposed for the etiology of sporadic prion diseases, including spontaneous somatic mutations in the *PRNP* gene or rare stochastic conformational changes in the structure of PrP^{C} (65). Whether the co-existent type 1 and type 2 PrP^{Sc} in sCJD is the result of such a primordial event or evolution in the passage through different cells expressing different post-translationally modified PrP^{C} remains to be established. When using new PrP^{C} substrate that may differ in primary sequence, post-translational modifications, or both, co-existent prions may undergo progressive conformational shifts due to the natural selection of the least stable conformers with the highest replication rate. Thus, the evolutionary conformational selection mechanism of PrP^{Sc} presented in this study may explain the recently observed acquisition of drug resistance by mammalian prions (66) and calls for the reevaluation of different therapeutic strategies targeting PrP^{Sc}. The high resolution structural tools and the study of the role of PrP^{Sc} ligands must address the apparent conformational plasticity of PrP^{Sc}, which is likely responsible for the natural selection process of prions and results in prion evolution and phenotypic diversity.

Acknowledgments—We are grateful to the patients' families, the CJD Foundation, and all the members of the National Prion Disease Pathology Surveillance Center. We thank Witold Surewicz for providing recombinant PrPs for CDI calibration and Earl Poptic from Cleveland Clinic Hybridoma Facility for scaled up production of mAb 8H4.

REFERENCES

1. Legname, G., Baskakov, I. V., Nguyen, H.-O., Riesner, D., Cohen, F. E., DeArmond, S. J., and Prusiner, S. B. (2004) Synthetic mammalian prions. *Science* **305,** 673–676
2. Deleault, N. R., Harris, B. T., Rees, J. R., and Supattapone, S. (2007) Formation of native prions from minimal components *in vitro*. *Proc. Natl. Acad. Sci. U.S.A.* **104,** 9741–9746
3. Wang, F., Wang, X., Yuan, C. G., and Ma, J. (2010) Generating a prion with bacterially expressed recombinant prion protein. *Science* **327,** 1132–1135
4. Prusiner, S. B. (1982) Novel proteinaceous infectious particles cause scrapie. *Science* **216,** 136–144
5. Safar, J. G. (2012) Molecular pathogenesis of sporadic prion diseases in man. *Prion* **6,** 108–115
6. Safar, J. G. (2012) in *Prions and Diseases* (Gambetti, P., ed) pp. 161–179, Springer-Verlag, New York
7. Bessen, R. A., and Marsh, R. F. (1994) Distinct PrP properties suggest the molecular basis of strain variation in transmissible mink encephalopathy. *J. Virol.* **68,** 7859–7868
8. Telling, G. C., Parchi, P., DeArmond, S. J., Cortelli, P., Montagna, P., Gabizon, R., Mastrianni, J., Lugaresi, E., Gambetti, P., and Prusiner, S. B. (1996) Evidence for the conformation of the pathologic isoform of the prion protein enciphering and propagating prion diversity. *Science* **274,** 2079–2082
9. Safar, J., and Prusiner, S. B. (1998) Molecular studies of prion diseases. *Prog. Brain Res.* **117,** 421–434
10. Li, J., Browning, S., Mahal, S. P., Oelschlegel, A. M., and Weissmann, C. (2010) Darwinian evolution of prions in cell culture. *Science* **327,** 869–872
11. Makarava, N., Savtchenko, R., and Baskakov, I. V. (2013) Selective amplification of classical and atypical prions using modified protein misfolding cyclic amplification. *J. Biol. Chem.* **288,** 33–41
12. Ghaemmaghami, S., Colby, D. W., Nguyen, H. O., Hayashi, S., Oehler, A., DeArmond, S. J., and Prusiner, S. B. (2013) Convergent replication of mouse synthetic prion strains. *Am. J. Pathol.* **182,** 866–874
13. Colby, D. W., Wain, R., Baskakov, I. V., Legname, G., Palmer, C. G., Nguyen, H. O., Lemus, A., Cohen, F. E., DeArmond, S. J., and Prusiner, S. B. (2010) Protease-sensitive synthetic prions. *PLoS Pathog.* **6,** e1000736
14. Puoti, G., Bizzi, A., Forloni, G., Safar, J. G., Tagliavini, F., and Gambetti, P. (2012) Sporadic human prion diseases: molecular insights and diagnosis. *Lancet Neurol.* **11,** 618–628
15. Kim, C., Haldiman, T., Surewicz, K., Cohen, Y., Chen, W., Blevins, J., Sy, M. S., Cohen, M., Kong, Q., Telling, G. C., Surewicz, W. K., and Safar, J. G. (2012) Small protease-sensitive oligomers of PrP(Sc) in distinct human prions determine conversion rate of PrP(C). *PLoS Pathog.* **8,** e1002835
16. Kim, C., Haldiman, T., Cohen, Y., Chen, W., Blevins, J., Sy, M. S., Cohen, M., and Safar, J. G. (2011) Protease-sensitive conformers in broad spectrum of distinct PrP structures in sporadic Creutzfeldt-Jakob disease are indicators of progression rate. *PLoS Pathog.* **7,** e1002242
17. Uro-Coste, E., Cassard, H., Simon, S., Lugan, S., Bilheude, J. M., Perret-Liaudet, A., Ironside, J. W., Haik, S., Basset-Leobon, C., Lacroux, C., Peoch, K., Streichenberger, N., Langeveld, J., Head, M. W., Grassi, J., Hauw, J. J., Schelcher, F., Delisle, M. B., and Andreoletti, O. (2008) Beyond PrP9res type 1/type 2 dichotomy in Creutzfeldt-Jakob disease. *PLoS Pathog.* **4,** e1000029
18. Yull, H. M., Ritchie, D. L., Langeveld, J. P., van Zijderveld, F. G., Bruce, M. E., Ironside, J. W., and Head, M. W. (2006) Detection of type 1 prion protein in variant Creutzfeldt-Jakob disease. *Am. J. Pathol.* **168,** 151–157
19. Schoch, G., Seeger, H., Bogousslavsky, J., Tolnay, M., Janzer, R. C., Aguzzi, A., and Glatzel, M. (2006) Analysis of prion strains by PrPSc profiling in sporadic Creutzfeldt-Jakob disease. *PLoS Med.* **3,** e14
20. Cali, I., Castellani, R., Alshekhlee, A., Cohen, Y., Blevins, J., Yuan, J., Langeveld, J. P., Parchi, P., Safar, J. G., Zou, W. Q., and Gambetti, P. (2009) Co-existence of scrapie prion protein types 1 and 2 in sporadic Creutzfeldt-Jakob disease: its effect on the phenotype and prion-type characteristics. *Brain* **132,** 2643–2658
21. Kobayashi, A., Mizukoshi, K., Iwasaki, Y., Miyata, H., Yoshida, Y., and Kitamoto, T. (2011) Co-occurrence of types 1 and 2 PrP(res) in sporadic Creutzfeldt-Jakob disease MM1. *Am. J. Pathol.* **178,** 1309–1315
22. Parchi, P., Giese, A., Capellari, S., Brown, P., Schulz-Schaeffer, W., Windl, O., Zerr, I., Budka, H., Kopp, N., Piccardo, P., Poser, S., Rojiani, A., Streichemberger, N., Julien, J., Vital, C., Ghetti, B., Gambetti, P., and Kretzschmar, H. (1999) Classification of sporadic Creutzfeldt-Jakob disease based on molecular and phenotypic analysis of 300 subjects. *Ann. Neurol.* **46,** 224–233
23. World Health Organization (1999) in *WHO Infection Control Guidelines for Transmissible Spongiform Encephalopathies* (Asher, D., and Pocchiari, M., eds) pp. 1–38, World Health Organization Emerging and Other Communicable Diseases, Geneva
24. Collins, S. J., Sanchez-Juan, P., Masters, C. L., Klug, G. M., van Duijn, C., Poleggi, A., Pocchiari, M., Almonti, S., Cuadrado-Corrales, N., de Pedro-Cuesta, J., Budka, H., Gelpi, E., Glatzel, M., Tolnay, M., Hewer, E., Zerr, I., Heinemann, U., Kretszchmar, H. A., Jansen, G. H., Olsen, E., Mitrova, E., Alpérovitch, A., Brandel, J. P., Mackenzie, J., Murray, K., and Will, R. G. (2006) Determinants of diagnostic investigation sensitivities across the clinical spectrum of sporadic Creutzfeldt-Jakob disease. *Brain* **129,** 2278–2287
25. Geschwind, M. D., Shu, H., Haman, A., Sejvar, J. J., and Miller, B. L. (2008) Rapidly progressive dementia. *Ann. Neurol.* **64,** 97–108

26. Parchi, P., Zou, W., Wang, W., Brown, P., Capellari, S., Ghetti, B., Kopp, N., Schulz-Schaeffer, W. J., Kretzschmar, H. A., Head, M. W., Ironside, J. W., Gambetti, P., and Chen, S. G. (2000) Genetic influence on the structural variations of the abnormal prion protein. *Proc. Natl. Acad. Sci. U.S.A.* **97,** 10168–10172
27. Parchi, P., Castellani, R., Capellari, S., Ghetti, B., Young, K., Chen, S. G., Farlow, M., Dickson, D. W., Sima, A. A., Trojanowski, J. Q., Petersen, R. B., and Gambetti, P. (1996) Molecular basis of phenotypic variability in sporadic Creutzfeldt-Jakob disease. *Ann. Neurol.* **39,** 767–778
28. Safar, J. G., Geschwind, M. D., Deering, C., Didorenko, S., Sattavat, M., Sanchez, H., Serban, A., Vey, M., Baron, H., Giles, K., Miller, B. L., Dearmond, S. J., and Prusiner, S. B. (2005) Diagnosis of human prion disease. *Proc. Natl. Acad. Sci. U.S.A.* **102,** 3501–3506
29. Langeveld, J. P., Jacobs, J. G., Erkens, J. H., Bossers, A., van Zijderveld, F. G., and van Keulen, L. J. (2006) Rapid and discriminatory diagnosis of scrapie and BSE in retro-pharyngeal lymph nodes of sheep. *BMC Vet. Res.* **2,** 19
30. Yuan, J., Xiao, X., McGeehan, J., Dong, Z., Cali, I., Fujioka, H., Kong, Q., Kneale, G., Gambetti, P., and Zou, W. Q. (2006) Insoluble aggregates and protease-resistant conformers of prion protein in uninfected human brains. *J. Biol. Chem.* **281,** 34848–34858
31. Choi, E. M., Geschwind, M. D., Deering, C., Pomeroy, K., Kuo, A., Miller, B. L., Safar, J. G., and Prusiner, S. B. (2009) Prion proteins in subpopulations of white blood cells from patients with sporadic Creutzfeldt-Jakob disease. *Lab. Invest.* **89,** 624–635
32. Zanusso, G., Liu, D., Ferrari, S., Hegyi, I., Yin, X., Aguzzi, A., Hornemann, S., Liemann, S., Glockshuber, R., Manson, J. C., Brown, P., Petersen, R. B., Gambetti, P., and Sy, M.-S. (1998) Prion protein expression in different species: Analysis with a panel of new mAbs. *Proc. Natl. Acad. Sci. U.S.A.* **95,** 8812–8816
33. Kascsak, R. J., Rubenstein, R., Merz, P. A., Tonna-DeMasi, M., Fersko, R., Carp, R. I., Wisniewski, H. M., and Diringer, H. (1987) Mouse polyclonal and monoclonal antibody to scrapie-associated fibril proteins. *J. Virol.* **61,** 3688–3693
34. Swietnicki, W., Morillas, M., Chen, S. G., Gambetti, P., and Surewicz, W. K. (2000) Aggregation and fibrillization of the recombinant human prion protein huPrP90–231. *Biochemistry* **39,** 424–431
35. Safar, J. G., Lessard, P., Tamgüney, G., Freyman, Y., Deering, C., Letessier, F., Dearmond, S. J., and Prusiner, S. B. (2008) Transmission and detection of prions in feces. *J. Infect. Dis.* **198,** 81–89
36. Safar, J. G., Scott, M., Monaghan, J., Deering, C., Didorenko, S., Vergara, J., Ball, H., Legname, G., Leclerc, E., Solforosi, L., Serban, H., Groth, D., Burton, D. R., Prusiner, S. B., and Williamson, R. A. (2002) Measuring prions causing bovine spongiform encephalopathy or chronic wasting disease by immunoassays and transgenic mice. *Nat. Biotechnol.* **20,** 1147–1150
37. Safar, J., Wille, H., Itri, V., Groth, D., Serban, H., Torchia, M., Cohen, F. E., and Prusiner, S. B. (1998) Eight prion strains have PrP^{Sc} molecules with different conformations. *Nat. Med.* **4,** 1157–1165
38. Thackray, A. M., Hopkins, L., and Bujdoso, R. (2007) Proteinase K-sensitive disease-associated ovine prion protein revealed by conformation-dependent immunoassay. *Biochem. J.* **401,** 475–483
39. Bellon, A., Seyfert-Brandt, W., Lang, W., Baron, H., Gröner, A., and Vey, M. (2003) Improved conformation-dependent immunoassay: suitability for human prion detection with enhanced sensitivity. *J. Gen. Virol.* **84,** 1921–1925
40. Choi, Y. P., Gröner, A., Ironside, J. W., and Head, M. W. (2011) Comparison of the level, distribution and form of disease-associated prion protein in variant and sporadic Creutzfeldt-Jakob diseased brain using conformation-dependent immunoassay and Western blot. *J. Gen. Virol.* **92,** 727–732
41. McCutcheon, S., Hunter, N., and Houston, F. (2005) Use of a new immunoassay to measure PrP Sc levels in scrapie-infected sheep brains reveals PrP genotype-specific differences. *J. Immunol. Methods* **298,** 119–128
42. Safar, J. G., Wille, H., Geschwind, M. D., Deering, C., Latawiec, D., Serban, A., King, D. J., Legname, G., Weisgraber, K. H., Mahley, R. W., Miller, B. L., Dearmond, S. J., and Prusiner, S. B. (2006) Human prions and plasma lipoproteins. *Proc. Natl. Acad. Sci. U.S.A.* **103,** 11312–11317
43. Safar, J., Roller, P. P., Gajdusek, D. C., and Gibbs, C. J., Jr. (1993) Conformational transitions, dissociation, and unfolding of scrapie amyloid (prion) protein. *J. Biol. Chem.* **268,** 20276–20284
44. Kong, Q., Huang, S., Zou, W., Vanegas, D., Wang, M., Wu, D., Yuan, J., Zheng, M., Bai, H., Deng, H., Chen, K., Jenny, A. L., O'Rourke, K., Belay, E. D., Schonberger, L. B., Petersen, R. B., Sy, M. S., Chen, S. G., and Gambetti, P. (2005) Chronic wasting disease of elk: transmissibility to humans examined by transgenic mouse models. *J. Neurosci.* **25,** 7944–7999
45. Fischer, M., Rülicke, T., Raeber, A., Sailer, A., Moser, M., Oesch, B., Brandner, S., Aguzzi, A., and Weissmann, C. (1996) Prion protein (PrP) with amino-proximal deletions restoring susceptibility of PrP knockout mice to scrapie. *EMBO J.* **15,** 1255–1264
46. Castilla, J., Morales, R., Saá, P., Barria, M., Gambetti, P., and Soto, C. (2008) Cell-free propagation of prion strains. *EMBO J.* **27,** 2557–2566
47. Notari, S., Capellari, S., Langeveld, J., Giese, A., Strammiello, R., Gambetti, P., Kretzschmar, H. A., and Parchi, P. (2007) A refined method for molecular typing reveals that co-occurrence of PrP(Sc) types in Creutzfeldt-Jakob disease is not the rule. *Lab. Invest.* **87,** 1103–1112
48. Pocchiari, M., Puopolo, M., Croes, E. A., Budka, H., Gelpi, E., Collins, S., Lewis, V., Sutcliffe, T., Guilivi, A., Delasnerie-Laupretre, N., Brandel, J. P., Alperovitch, A., Zerr, I., Poser, S., Kretzschmar, H. A., Ladogana, A., Rietvald, I., Mitrova, E., Martinez-Martin, P., de Pedro-Cuesta, J., Glatzel, M., Aguzzi, A., Cooper, S., Mackenzie, J., van Duijn, C. M., and Will, R. G. (2004) Predictors of survival in sporadic Creutzfeldt-Jakob disease and other human transmissible spongiform encephalopathies. *Brain* **127,** 2348–2359
49. Gambetti, P., Kong, Q., Zou, W., Parchi, P., and Chen, S. G. (2003) Sporadic and familial CJD: classification and characterisation. *Br. Med. Bull.* **66,** 213–239
50. Telling, G. C., Scott, M., Mastrianni, J., Gabizon, R., Torchia, M., Cohen, F. E., DeArmond, S. J., and Prusiner, S. B. (1995) Prion propagation in mice expressing human and chimeric PrP transgenes implicates the interaction of cellular PrP with another protein. *Cell* **83,** 79–90
51. Steensgaard, J., Humphries, S., and Spragg, S. P. (1992) in *Preparative Centrifugation: A Practical Approach* (Rickwood, D., ed) pp. 187–232, IRL Press at Oxford University Press, Oxford
52. Kimberlin, R. H., and Walker, C. A. (1978) Evidence that the transmission of one source of scrapie agent to hamsters involves separation of agent strains from a mixture. *J. Gen. Virol.* **39,** 487–496
53. Bruce, M. E., and Fraser, H. (1991) Scrapie strain variation and its implications. *Curr. Top. Microbiol. Immunol.* **172,** 125–138
54. Bruce, M. E. (1993) Scrapie strain variation and mutation. *Br. Med. Bull.* **49,** 822–838
55. Bessen, R. A., and Marsh, R. F. (1992) Identification of two biologically distinct strains of transmissible mink encephalopathy in hamsters. *J. Gen. Virol.* **73,** 329–334
56. Bessen, R. A., and Marsh, R. F. (1992) Biochemical and physical properties of the prion protein from two strains of the transmissible mink encephalopathy agent. *J. Virol.* **66,** 2096–2101
57. Scott, M. R., Peretz, D., Nguyen, H.-O., Dearmond, S. J., and Prusiner, S. B. (2005) Transmission barriers for bovine, ovine, and human prions in transgenic mice. *J. Virol.* **79,** 5259–5271
58. Scott, M., Peretz, D., Ridley, R. M., Baker, H. F., DeArmond, S. J., and Prusiner, S. B. (2004) in *Prion Biology and Diseases* (Prusiner, S. B., ed) 2nd Ed., pp. 435–482, Cold Spring Harbor Laboratory Press, Cold Spring Harbor, NY
59. Bishop, M. T., Will, R. G., and Manson, J. C. (2010) Defining sporadic Creutzfeldt-Jakob disease strains and their transmission properties. *Proc. Natl. Acad. Sci. U.S.A.* **107,** 12005–12010
60. Korth, C., Kaneko, K., Groth, D., Heye, N., Telling, G., Mastrianni, J., Parchi, P., Gambetti, P., Will, R., Ironside, J., Heinrich, C., Tremblay, P., DeArmond, S. J., and Prusiner, S. B. (2003) Abbreviated incubation times for human prions in mice expressing a chimeric mouse—human prion protein transgene. *Proc. Natl. Acad. Sci. U.S.A.* **100,** 4784–4789
61. Manuelidis, L., and Lu, Z. Y. (2003) Virus-like interference in the latency and prevention of Creutzfeldt-Jakob disease. *Proc. Natl. Acad. Sci. U.S.A.* **100,** 5360–5365
62. Bartz, J. C., Kramer, M. L., Sheehan, M. H., Hutter, J. A., Ayers, J. I., Bessen,

R. A., and Kincaid, A. E. (2007) Prion interference is due to a reduction in strain-specific PrPSc levels. *J. Virol.* **81,** 689–697
63. Shikiya, R. A., Ayers, J. I., Schutt, C. R., Kincaid, A. E., and Bartz, J. C. (2010) Coinfecting prion strains compete for a limiting cellular resource. *J. Virol.* **84,** 5706–5714
64. Piro, J. R., Harris, B. T., Nishina, K., Soto, C., Morales, R., Rees, J. R., and Supattapone, S. (2009) Prion protein glycosylation is not required for strain-specific neurotropism. *J. Virol.* **83,** 5321–5328
65. Prusiner, S. B. (2001) Shattuck Lecture—Neurodegenerative diseases and prions. *N. Engl. J. Med.* **344,** 1516–1526
66. Oelschlegel, A. M., and Weissmann, C. (2013) Acquisition of drug resistance and dependence by prions. *PLoS Pathog.* **9,** e1003158